Geosci. Model Dev. Discuss., 8, 8547–8606, 2015
www.geosci-model-dev-discuss.net/8/8547/2015/
doi:10.5194/gmdd-8-8547-2015

Geoscientific Model Development Discussions
Open Access

Determining lake surface water temperatures (LSWTs) worldwide using a tuned 1-dimensional lake model (*FLake*, v1)

A. Layden[1], S. MacCallum[2], and C. Merchant[3]

[1]4 Rose Hill, Sligo, Ireland
[2]The University of Edinburgh, School of Geosciences, Grant Institute, The King's Buildings, West Mains Road, Edinburgh EH9 3FE, UK
[3]Dept. of Meteorology, University of Reading Harry Pitt Building, 3 Earley Gate, P.O. Box 238, Whiteknights, Reading, RG6 6AL, UK

Received: 20 July 2015 – Accepted: 27 July 2015 – Published: 8 October 2015

Correspondence to: A. Layden (aislinglayden99@gmail.com)

Published by Copernicus Publications on behalf of the European Geosciences Union.

Abstract

FLake, a 1-dimensional freshwater lake model, is tuned for 244 globally distributed large lakes using lake surface water temperatures (LSWTs) derived from Along-Track Scanning Radiometers (ATSRs). The model, tuned using only 3 lake properties; lake depth, albedo (snow and ice) and light extinction co-efficient, substantially improves the measured biases in various features of the LSWT annual cycle, including the LSWTs of saline and high altitude lakes. The daily mean absolute differences (MAD) and the spread of differences (±2 standard deviations) across the trial seasonally ice covered lakes (lakes with a lake-mean LSWT remaining below 1 °C for part of the annual cycle) is reduced from 3.01 ± 2.25 °C (pre-tuning) to 0.84 ± 0.51 °C (post-tuning). For non-seasonally ice-covered trial lakes (lakes with a lake-mean LSWT remaining above 1 °C throughout its annual cycle), the average daily mean absolute difference (MAD) is reduced from 3.55 ± 3.20 °C to 0.96 ± 0.63 °C. The post tuning results for the trial lakes (35 lakes) are highly representative of the post tuning results of the 244 lakes.

The sensitivity of the summer LSWTs of deeper lakes to changes in the timing of ice-off is demonstrated. The modelled summer LSWT response to changes in ice-off timing is found to be strongly affected by lake depth and latitude, explaining 0.50 (R^2_{adj}, $p = 0.001$) of the inter-lake variance in summer LSWTs. Lake depth alone explains 0.35 ($p = 0.003$) of the variance. The tuning approach undertaken in this study, overcomes the obstacle of the lack of available lake characteristic information (snow and ice albedo and light extinction co-efficient) for individual lakes. Furthermore, the tuned values for lake depth, snow and ice albedo and light extinction co-efficient for the 244 lakes provide guidance for improving LSWTs modelling in *FLake*.

1 Introduction

The response of LSWTs to climate is highly variable and is influenced by lake physical characteristics (Brown and Duguay, 2010). Some large lakes have been shown to alter the local climate. The extent of ice cover on lakes is considered to be a sensitive indicator of and also a factor in global change (Launiainen and Cheng, 1998). Changes in the length of the ice cover period affect local climatic feedbacks, for example, a shorter ice cover period allows for a longer time for surface heat exchange with the atmosphere (Ashton, 1986). This is of particular importance in areas where there is a high concentration of lakes, such as Canada (Pour et al., 2012). The large Canadian lakes of Great Bear and Great Slave can alter the local climate through lake-effect storms, impacting on the fluxes of heat, moisture, and momentum, and on the mesoscale weather processes (Long et al., 2007). Shallow lakes, particularly those with a large surface area, such as Lake Balaton, are more sensitive to atmospheric events (Voros et al., 2010).

Reliable modelling of LSWTs can enrich our understanding of the highly variable dynamic nature of lakes. In this paper, a 1-dimensional freshwater lake model, *FLake* (available at http://www.flake.igb-berlin.de/sourcecodes.shtml), is tuned with ATSR Reprocessing for Climate: Lake Surface Water Temperature and Ice Cover (ARC-Lake) observations (MacCallum and Merchant, 2012) of 244 globally distributed lakes. The tuned model is expected to improve the representation of these lakes in *FLake*.

There have been some modelling studies carried out that use both the *FLake* model and LSWT observations on European lakes (Voros et al., 2010; Bernhardt et al., 2012; Pour et al., 2012). The findings of two of these three studies show consistent biases between the modelled and observed LSWTs (overestimation of the open water LSWTs and underestimation of the ice cover period). Despite these biases, *FLake* is considered to be a reliable model for studying LSWTs and ice phenology and is considered suitable for global application for ice covered lakes (Bernhardt et al., 2012). These modelled biases (overestimation of the open water LSWTs and underestimation of the ice cover period) are consistent with findings from preliminary trial work carried out in this

GMDD
8, 8547–8606, 2015

study, which included North American and European lakes. It is the intention of this tuning study to achieve an average daily mean absolute difference (MAD) of $\leq 1\,^{\circ}$C, across all lakes. An average MAD of $\leq 1\,^{\circ}$C is possibly accurate enough for a global scale study mean. A lower MAD target may not be achievable as this study comprises of lakes with a wide range of geographical and physical characteristics.

Many lake specific properties can be considered in *FLake.* Through preliminary model trials, three properties; lake depth (d), albedo; snow and ice (α) and light extinction coefficient (κ) are shown to greatly influence the modelled LSWT cycle. Furthermore, optimal values for these three properties (herein referred to LSWT regulating properties) are shown to greatly improve the LSWT modelling in *FLake*.

An example of the preliminary trial work is shown for Lake Athabasca, in Fig. 1a. In this figure, a greater modelled α (higher reflectivity) results in a later ice-off date than the default model albedo and is closely comparable to the observed ice-off date. In Fig. 1b, it is demonstrated that by using a lower d than the mean depth of the lake, the ice-on day occurs earlier and corresponds more closely to the observed ice-on day. The modelled LSWT is further improved, by lowering the κ value (greater transparency). The greater transmission of surface heat to the lower layers result in a lower and more representative maximum LSWT, Fig. 1b. The LSWTs modelled using a combination of the greater α, lower d and lower κ compare closely with the observed LSWTs, Fig. 1c.

In this study, for each lake, the modelled biases for several features in the LSWT annual cycle are measured, quantifying the level of agreement with observed LSWTs. These modelled biases are the basis for selecting the tuned (optimal) LSWT regulating properties (d, α and κ) for each lake. Lakes are divided into 2 distinct categories. Lakes with a lake-mean LSWT climatology (determined using twice-a-month ARC-Lake full year LSWT observations, 1992/1996–2011) remaining below $1\,^{\circ}$C for part of the seasonally cycle are referred to as seasonally ice covered lakes (160 lakes). All other lakes are referred to as non-seasonally ice covered lakes (86 lakes). Although some of the seasonally ice covered lakes may not be completely ice covered during the cold season and some of the non-seasonally ice covered lakes may have short periods of partial ice cover, the 1 °C lake-mean LSWT offers a good means of evaluating lakes that are typically and non-typically ice covered during the coldest part of the LSWT cycle. To capture the critical features in the LSWT cycle, the biases quantified differ for the 2 lake categories.

2 Methods

2.1 Data; ARC-Lake observed LSWTs

The ARC-Lake LSWT observations for 246 globally distributed large lakes, principally those with surface area > 500 km^2 (Herdendorf, 1982; Lehner and Doll, 2004) but includes 28 globally distributed smaller lakes, the smallest of which is 100 km^2 (Lake Vesijarvi) are used to tune the model. These LSWTs are generated from three Along-Track Scanning Radiometers (ATSRs), from 1991–2011 (MacCallum and Merchant, 2012). A synopsis of the derivation and validation of these observations is available in Layden et al. (2015).

The ARC-Lake observations have been shown to compare well with in situ LSWT data. Validation of the observations was performed through a match-up data set of in situ temperature data consisting of 52 observation locations covering 18 of the lakes (MacCallum and Merchant, 2012). Furthermore, the 1 °C cooling and warming day, which is defined as the day of the year on which the average (over the period of observations) lake-mean LSWT drops to below 1 °C (1 °C cooling day) and rises to above 1 °C (1 °C warming day), show a good consistency with in situ measurements of ice-on and ice-off days for 21 Eurasian and North American lakes (Layden et al., 2015). Layden et al. (2015) also demonstrates the integrity of the ARC-Lake LSWTs on a global scale, through the strong relationship between the observed LSWTs and meteorological data (features of air temperature and solar radiation) and geographical features (latitude and altitude). On this basis, the ARC-Lake LSWTs are considered reliable and suitable for use in this tuning study.

GMDD
8, 8547–8606, 2015

An average of the day and night lake-mean LSWT observations from August 1991 to the end of 2010 are used to tune the model, retaining the final year of observations (2011) to carry out an independent evaluation on the tuned model. For 119 lakes, there are continuous LSWT observations for 20 years (all three ATSR instruments, from August 1991 to December 2011), 113 lakes have 16 years of continuous LSWT observations (2 ATSR instruments), and 14 lakes have 8–9 years of LSWT observations (1 ATSR instrument). The location of the 246 lakes (55° S to 69° N), classified by surface area, is shown in Fig. 2.

2.2 Model; *FLake* lake model

FLake is a 1-dimensional thermodynamic lake model, capable of predicting the vertical temperature structure and mixing conditions of a lake. This model is a two-layer parametric representation of the evolving temperature profile of a lake and is based on the net energy budgets (Mironow, 2008). The lake conditions of the homogeneous "upper mixed layer" (epilimnion) and the "bottom layer" as represented in Fig. 3, are modelled in *FLake*. *FLake* utilises the minimum set of input data required for 1-dimensional thermal and ice models; meteorological forcing data (shortwave and long wave radiation, wind speed, air vapour pressure and air temperature), an estimation of turbidity and basic bathymetric data (Lerman et al., 1995). In *FLake*, the thermocline is parameterised through a self-similarity representation of the temperature profile. Although, models based on the concept of self-similarity are considered to be only fairly accurate (Dutra et al., 2010), we show that modelled biases are greatly reduced by tuning the model.

2.2.1 Lake specific model properties

As outlined in the introduction, optimisation of LSWT regulating properties; lake depth (d), albedo; snow and ice (α) and light extinction coefficient (κ), can greatly improve the LSWTs produced in *FLake*. Values for other lake-specific properties outlined in this section are retained throughout the investigative and tuning process.

GMDD
8, 8547–8606, 2015

c_relax_C; is a relaxation time scale for the temperature profile in the thermocline. The default c_relax_C value of 0.003 was found to be too low to adequately readjust the temperature profile of deep lakes (G. Kirillin, personal communication, 2010), weakening the predicted stratification and affecting the LSWT. For lakes with mean depths < 5 m, the c_relax_C is set to 10^{-2}, and decreases with increasing depth, to a setting of 10^{-5} for mean depths > 50 m, as recommended by G. Kirillin (personal communication, 2010).

fetch; wind fetch is calculated as the square root of the product of lake length and breadth measurements. These measurements are available for 205 of the 246 lakes. The calculated fetch of these 205 lakes are found to be strongly related to surface area, Eq. (1), $R^2_{adj} = 0.84, p = 0.001$. Equation (1) is used to determine the fetch of the remaining 41 lakes with no available dimensions.

$$\text{fetch} = 39.9 + 0.00781\ \text{area} \tag{1}$$

latitude; the latitude of the lake centre reference co-ordinates (Herdendorf, 1982; Lehner and Doll, 2004).

Starting conditions; these provide *FLake* with the lake specific initial temperature and mixing conditions. Other than shortening the model spin-up time, the starting conditions showed no influence over the modelled LSWTs thereafter. The starting conditions are temperature of upper mixed layer, bottom temperature, mixed layer depth, ice thickness and temperature at air–ice interface. A good estimation of the starting conditions for each lake was obtained from the *FLake* model based on the hydrological year 2005/06 (Kirillin et al., 2011).

2.2.2 Fixed model parameters

The model parameters that remain fixed throughout the investigative and tuning process, across all lakes (fixed model parameters) are icewater_flux, inflow from the catchment, heat flux from sediments and variation in the light extinction coefficient.

GMDD
8, 8547–8606, 2015

For icewater_flux, (heat flow from water to ice) G. Kirillin (personal communication, 2010) suggests values of ~ 3–$5\,\mathrm{W\,m^2}$. In this study a value of $5\,\mathrm{W\,m^2}$ is applied to all lakes. The inflow from the catchment and heat flux from sediments are not considered in this study. Variation (throughout the annual cycle) of light extinction coefficient is not considered. However, the effect of light extinction coefficient on LSWT, when its effect is most prominent (summer time) is considered, as discussed in Sect. 2.4.

2.2.3 Model forcing data

FLake is forced with ECMWF Interim Re-analysis (ERA) data (Dee et al., 2011; ECMWF, 2009), at the grid points closest to the lake centre ($0.7^\circ \times 0.7^\circ$ resolution), as shown in the Supplement. Shortwave solar downward radiation (SSRD), air temperature and vapour pressure at 2 m, wind speed and total cloud cover, in their mean daily values, as shown in Table 1 are used to force the model.

As most long-term wind speed records are measured over land (U_{land}) and are considered to underestimate the wind speed over water (U_{water}), scaling of the wind speeds is considered during the trials. For water bodies with fetches > 16 m, Hsu (1988) recommends the scaling shown in Eq. (2). For bodies of water with fetch < 16 m a scaling of 1.2 is considered reasonable (Resio et al., 2003). To find a suitable wind speed scaling, the trial work is carried out using the unscaled wind speed (*u1*), wind speed factored by 1.2 (*u2*), and wind speed suggested by Hsu (1988), *u3* (Eq. 2).

$$U_{\mathrm{water}} = 1.62 + 1.17 U_{\mathrm{land}} \tag{2}$$

2.3 Tuning method

A suitable range of factors/values for d, κ and α is determined through the model trials (carried out on 21 seasonally ice covered and 14 non-seasonally ice covered lakes, Fig. 4).

The lakes used in the trials are chosen because they broadly represent the range of lake characteristics – lake depth, albedo and light extinction coefficient – and have available Secchi disk depth data. Secchi disk depth data is used to derive light extinction coefficients values in the first trial (untuned model).

2.3.1 Light extinction coefficients for trial lakes

The light extinction coefficients values for the untuned model trial are derived from Secchi disk depth data (κ_{sd}), obtained from the ILEC database (ILEC, 1999). Many studies have been carried out deriving κ values from Secchi disk depths (Poole and Atkins, 1929; Holmes, 1970; Bukata et al., 1988; Monson, 1992; Armengol et al., 2003). Five methods of relating κ values to Secchi disk depths are compared in Fig. 5. This comparison covers a range of different water conditions, from coastal turbid waters (Holmes, 1970) and eutrophic water (tested 1 km from a dam in the Sau reservoir, Spain) (Armengol et al., 2003) to a range of North American lakes of different trophic levels (Monson, 1992).

For Secchi disk depths > 10 m, as shown in Fig. 5, all methods show a good comparison between Secchi disk depths and κ. From Secchi disk depths of 10 to 1 m the range of results between studies become increasingly large. Bukata et al. (1998) showed that the formula Eq. (3), based on in situ optical measurements from many stations, adequately described Lake Huron, Lake Superior and Lake Ontario, for Secchi disk depths from 2 to 10 m;

$$\kappa_{sd} = 0.757 \times S^{-1} + 0.07 \tag{3}$$

where S^{-1} = inverse Secchi disk depth (m). Of the 5 studies, this formula produces the lowest (most transparent) κ values, and possibly more likely to represent open water conditions of large lakes and is therefore used in this study.

For Secchi disk depths outside the 2–10 m range (less than 2 m and greater than 10 m) the Poole and Atkins (1929) formula is applied. This formula, Eq. (4), is used as it is considered to serve as a universal relation between light extinction coefficient and Secchi disk depth data and provides sufficiently accurate estimations of light extinction

GMDD
8, 8547–8606, 2015

coefficients in waters with all degrees of turbidity (Sherwood, 1974).

$$\kappa_{sd} = 1.7\ /\text{Secchi disk depth} \tag{4}$$

2.3.2 Light extinction coefficients for tuning of all lakes

Many lakes do not have available Secchi disk depth data. For this reason, an alternative approach is used to provide light extinction coefficients in the tuned model trials and for the tuning of all lakes. A range of 10 optical water types which essentially describe the attenuation process of oceans and its changes with turbidity (Jerlov, 1976) is applied. These consist of 5 optical water types for open ocean, type I, IA, IB, II and III; type I being the most transparent and type III being least transparent and 5 coastal ocean types (1, 3, 5, 7 and 9) (Jerlov, 1976). The spectra for these 10 ocean types are divided (0.18, 0.54, 0.28) into three wavelengths; 375, 475 and 700 nm, respectively. The 10 ocean types are renamed herein as κ_{d1} to κ_{d10} the values for which are shown in Table 2.

2.3.3 Tuning of lake depth

Lake depth information was obtained from Herdendorf (1982), the ILEC World Lake Database (http://wldb.ilec.or.jp/), LakeNet (http://www.worldlakes.org/) and (Kourzeneva et al., 2012). The mean depth (Z_d1) is the recommended depth value for *FLake*. Where only maximum depth is available (9 lakes), the mean depth is calculated using the average maximum-to-mean depth ratio of lakes with known maximum and mean depths. This ratio is 3.5 for seasonally ice covered lakes and 3.0 for non-seasonally ice covered lakes. Effective depth (Z_d) factors are applied to the lake-mean depth ($Z_d1 : Z_d6$), resulting in lake depths ranging from 0.3 to 2.5 times the mean depth, Table 2. For lakes with no depth information, the effective depth factors are applied to an initial depth of 5 m. If a low depth is indicated (early LSWT cooling and/or a high LSWT comparative to observed LSWT), tuning is repeated using a greater input depth.

2.3.4 Tuning of snow and ice albedo

The model default albedo (α) value is 0.60 for snow and white ice and 0.10 for melting snow and blue ice, referred to as $\alpha 1$. On the basis of the modelled biases outlined in the introduction, we apply 3 additional albedos of higher values ($\alpha 2:\alpha 4$), shown in Table 2, when tuning of seasonally ice-covered lakes. A higher albedo causes more of the incoming radiation to be reflected, causing a later (and more timely) ice-off. Albedo when discussed throughout this study refers to snow and ice albedo.

2.3.5 Wind speed scaling

Trial work is carried out using the unscaled wind speed (*u1*) and scaled wind speeds, *u2* and *u3,* as described in Sect. 2.2.3. During the trial work, the most appropriate wind speed scalings are determined and are subsequently used in the tuning study.

2.3.6 Summary of the tuning of the LSWT regulating properties

Table 2 contains a summary of the factors/values for d, κ and α used in the tuning study. The tuning approach applied in this study provides an effective method for the tuning of LSWTs and overcomes the limitation of the lack of available lake characteristic information for many lakes. The model is tuned using the optimal combination of LSWT regulating properties; 80 possible combinations for seasonally ice covered lakes and 60 possible combinations for non-seasonally ice covered lakes.

2.4 Tuning metrics

The tuning metrics are the biases (between the modelled and the observed LSWTs) which are used to quantify the effect that the LSWT regulating properties have on the modelled LSWTs.

GMDD
8, 8547–8606, 2015

2.4.1 Tuning metrics for seasonally ice covered lakes

The metrics and the effect of the LSWT regulating properties on them, for seasonally ice covered lakes is summarised in Table 3. The light extinction co-efficient effect on the summertime LSWT; July, August and September (JAS) LSWT is demonstrated in Fig. 6, showing that the tuned κ_d value (κ_{d6}) substantially improves the JAS LSWT. The effect that the tuned lake depth has on the 1 °C cooling day (the day the lake-mean LSWT drops below 1 °C; an indicator of ice-on) is demonstrated in Fig. 7. The 1 °C warming day is the day the lake-mean LSWT rises to above 1 °C; an indicator of ice-off). The daily MAD measures the daily mean absolute difference between the modelled and observed LSWTs. The closeness of the modelled and observed LSWTs is measured using these 4 metrics (normalized and equally weighted) and are the basis of selecting the optimal LSWT model for each lake.

2.4.2 Tuning metrics for non-seasonally ice covered lakes

The metrics for non-seasonally ice covered lakes are more difficult to ascertain, as there are no definitive stages in the LSWT cycle. For these lakes, the difference between the observations and model for the months where the minimum and maximum LSWTs occur ($\mathrm{mth}_{\mathrm{min}}$ and $\mathrm{mth}_{\mathrm{max}}$) are applied as metrics. These metrics exert some control over temporally reconciling the observed and modelled monthly extremes. The daily MAD is also used to measure the daily mean absolute difference between the modelled and observed LSWTs.

2.4.3 Additional metrics for seasonally and non-seasonally ice covered lakes

The fraction of the observed LSWT variance that is accounted for in the tuned model is used to help independently evaluate the tuned LSWTs. For the observed LSWTs, over the length of the tuning period, the variance (K^2) in the month of minimum and maximum LSWT for non-seasonally ice covered lakes ($\mathrm{var}_{\mathrm{min}}$ and $\mathrm{var}_{\mathrm{max}}$) and in the

GMDD
8, 8547–8606, 2015

JAS LSWT for seasonally ice covered lakes (var_{jas}) is determined. The fraction of these observed LSWT variances accounted for in the tuned model are quantified, $inter_{min}$, $inter_{max}$ and $inter_{jas}$ (R^2_{adj}), respectively. The calculations to quantify var_{jas} and $Inter_{jas}$ are shown in Eqs. (5) and (6).

var_{jas} (K^2) observed JAS LSWT variance;

$$var_{jas} = \sum (x_i^{obs\_jas} - \bar{x})^2/(N-1) \quad (5)$$

where obs_jas = observed JAS LSWT. $Inter_{jas}$ (R^2_{adj}); the fraction of the observed JAS LSWT inter-annual variance accounted for in the tuned model;

$$inter_{jas} = 1 - ((1-r^2)(N-1)/(N-P-1)) \quad (6)$$

N = sample size (number of years with JAS LSWTs)
P = total number of regressors

$$r^2 = \frac{N\sum\left(x_i^{obs\_jas} x_i^{mod\_jas}\right) - \sum\left(x_i^{obs\_jas}\right)\sum\left(x_i^{mod\_jas}\right)}{\left(N\sum\left(x_i^{mod\_jas2}\right) - \sum\left(x_i^{mod\_jas}\right)^2\right)\left(N\sum\left(x_i^{obs\_jas2}\right) - \sum\left(x_i^{obs\_jas}\right)^2\right)}$$

where mod_jas = modelled JAS LSWT. The same Eqs. (5) and (6) are applied to determine $Inter_{max}$, var_{max}, $Inter_{min}$ and var_{min}, substituting "JAS" with "max" and "min".

2.4.4 Overview of tuning method

An overview of tuning approach for seasonally and non-seasonally ice covered lakes is shown in Fig. 8.

3 Applied wind speeds

Wind speed was examined in the untuned model trial for both seasonally and non-seasonally ice covered lakes. The trials show that wind speed has a consistent effect on the modelled LSWT of seasonally ice covered lakes. The higher wind speed scaling (*u3*) causes an earlier (and more timely) cooling and later (and more timely) warming, lengthening the ice cover period, as demonstrated for Lake Simcoe in Fig. 9. The more rapid mixing and heat exchange between the surface and atmosphere, as a result of the higher wind speed, causes an earlier modelled 1 °C cooling day. As wind promotes ice growth in the model, higher wind speeds also contribute to the later modelled 1 °C warming day. Wind speed scaling, *u3* in place of *u1*, for the trial seasonally ice covered lakes, reduces the bias in the length of the average cold phase (when compared to the observed cold phase) by ~ half (from 39 to 21 days) and reduces the JAS (July, August, September) LSWT bias by ~ half, from 3.71 to 1.87 °C, Table 4. On this basis of these trial results, the higher wind speed scaling, *u3* ($U_{\text{water}} = 1.62 + 1.17U_{\text{land}}$) is applied to all seasonally ice covered lakes.

For non-seasonally ice covered trial lakes, 5 of the 7 lakes at latitudes > 35° N/S show best results with *u3*, as demonstrated for a lake located at 35.6° N, Fig. 10a. Five (5) of the 7 lakes located < 35° N/S show best results with *u1*, as demonstrated for a lake located at 3.5° N, Fig. 10b. Of the scalings applied, there is no optimal wind speed scaling for all non-seasonally ice covered lakes. This may be attributable to the highly variable range of latitudes, LSWTs and mixing regimes of non-seasonally ice covered lakes.

For the remainder of the trials (tuned), wind speed scaling *u1*, was applied to lakes at latitudes < 35° N/S and *u3* to lakes at latitudes > 35° N/S for non-seasonally ice covered lakes. The metrics from the final set of trials (tuned using the range of d, κ and α factors/values outlined in Table 2) are shown in the second results column in Table 5. For both seasonally and non-seasonally ice covered lakes, the target average MAD of < 1.0 °C is achieved for the trial lakes. As a result, this tuning approach is applied to all lakes.

4 Results

4.1 Summary of results

The average MAD and spread of differences (2σ) for seasonally and non-seasonally ice covered lakes, is reduced from 3.07 ± 2.55 and $3.55 \pm 3.20\,^{\circ}$C for the untuned model to 0.96 ± 0.63 and $0.84 \pm 0.51\,^{\circ}$C for the tuned model, Table 5. These results demonstrate that the untuned model, run using the lake mean depth, light extinction coefficients derived from Secchi disk depth (as shown in Sect. 2.3.1) and default the model default albedo (seasonally ice covered lakes only) can be greatly improved by the tuning process with the applied wind speed scalings.

The tuning method applied to seasonally ice covered lakes is shown to be suitable for 135 of the 160 lakes, yielding an average MAD of $0.74 \pm 0.48\,^{\circ}$C, Table 6. The remaining 25 seasonally ice covered lakes yielded comparatively poor results. These 25 lakes were re-tuned using higher d factors and higher κ_d values, as outlined in the next sub-section (Sect. 4.1.1), yielding an average daily MAD of $1.11 + 0.56\,^{\circ}$C. Across the 160 lakes, an average MAD ($0.80 \pm 0.56\,^{\circ}$C, Table 5), of below $1\,^{\circ}$C was achieved.

For non-seasonally ice covered lakes, the average daily MAD result for 84 of the 86 lakes is $0.96\,^{\circ}$C, with a spread of differences of $\pm 0.66\,^{\circ}$C (2σ), Table 5, achieving an average MAD of below $1\,^{\circ}$C. Two of the 86 lakes yield highly unsatisfactory results.

The tuned values for the LSWT regulating properties for all lakes and the tuning metrics are shown in the Supplement.

4.1.1 Seasonally ice covered lakes

The average tuned metrics for 135 of the 160 lakes and the trial lakes are highly comparable, Table 6. For the remaining 25 lakes, the tuned metrics are comparatively poor; the $1\,^{\circ}$C cooling day was ≥ 14 days too early and/or the JAS LSWT value was $\geq 2\,^{\circ}$C. These 25 shallow lakes (average depth < 5 m) were tuned to the highest depth factor, Z_{d4} and/or the highest light extinction coefficient, κ_{d5} (lowest transparency). Although

GMDD
8, 8547–8606, 2015

Determining LSWTs worldwide

A. Layden et al.

the transparencies for these 25 lakes are largely unknown, shallow lakes generally have poorer light transparencies than deeper lakes due to upwelling of bottom sediment. The shallow depth of the modelled lake (lower heat capacity) and the poor transparency of water (more heat retained in surface) were evident in the metric results; early 1 °C cooling day and/or high JAS LSWT values. This indicates that the these lakes require a greater modelled depth to increase the heat capacity, postponing the 1 °C cooling day and lower transparency values (higher κ_d) causing less heat to be retained in the surface, decreasing the JAS LSWT. A tuning modification, using 3 greater depth factors, $Z_{d5} : Z_{d7}$, and 2 higher light extinction coefficient values, κ_{d6} and κ_{d7} (Table 2) is applied. This modification substantially improves the 1 °C cooling day and the JAS LSWT for these 25 lakes. A summary of the results are shown in Table 6 column 2. The tuning metrics results for the 160 lakes (using the modified set-up for the 25 shallow lakes) are illustrated in Fig. 11.

4.1.2 Non-seasonally ice covered lakes

The tuning metrics results for each of the 84 lakes are illustrated in Fig. 12 and a summary of these results are shown in Table 5.

For 2 of the 86 lakes, Lake Viedma and the Dead Sea, the difference between the altitude of the ERA T2 air temperature (geopotential height) and the lake altitude is the most possible cause for poor tuning results. Lake Viedma, an Argentinian freshwater lake of unknown depth yielded a daily MAD of 3.1 °C and The Dead Sea, a deep and highly saline lake (340 $\mathrm{g\,L^{-1}}$) located in Asia at 404 m below sea level yielded a daily MAD of 4.1 °C. For the Dead Sea, a difference in the month of maximum temperature between the observed LSWT (33 °C) and ERA T2 air temperature (25 °C), results in a negative modelled bias of 6.3 °C in the month of maximum LSWT. Given the standard air temperature lapse rate (6.5 $\mathrm{°C\,km^{-1}}$), altitude can explain the substantially lower air temperatures. The altitude of Dead Sea (–404 m a.s.l.), is lower by ~ 850 m a.s.l. than the altitude of the meteorological data at the lake centre co-ordinates, 445 m a.s.l.

(determined by interpolating surrounding cells using the orography data accompanying the ECMWF meteorological data).

For Lake Viedma, while the observed LSWTs range from 5–10 °C, the minimum ERA T2 air temperature remains well below 0 °C for many months of year, regularly reaching −8 °C, resulting in the negative modelled bias of 4.8 °C in the month of minimum LSWT. This bias can be at least, partially explained by the difference in altitude of > 500 m a.s.l., between the altitude of Lake Viedma (297 m a.s.l.) and the altitude of meteorological data at the lake centre co-ordinates of 825 m a.s.l.

4.2 Tuning of saline and high altitude lakes

The tuning of *FLake* is successful for both saline and high altitude lakes, as well as freshwater and low altitude lakes, as shown in Table 7 (seasonally ice covered lakes) and in Table 8 (non-seasonally ice covered lakes).

The density of freshwater in *FLake* is determined at sea level (normal atmospheric pressure) (Mironow, 2008). At higher altitudes, the lower water density results in less effective natural convective and thermal heat transfer processes. Although lake altitude is not considered in *FLake*, the effect of altitude (ranging from −12 to 5000 m a.s.l.,) on LSWT is shown to be minimal or else compensated for by the tuning process. The majority of the high altitude lakes are also saline; 7 of the 10 non-seasonally ice covered lakes and 12 of the 14 seasonally ice covered lakes. The comparability between observed and modelled LSWTs for two high altitude lakes (> 1500 m a.s.l.) are shown in Fig. 13.

4.3 Independent evaluation

Two methods are used to independently evaluate the tuned model.

1. The fraction of observed LSWT variance that is detected in the tuned model is quantified.

GMDD
8, 8547–8606, 2015

2. The metrics for 2011 (observed LSWTs from 2011 were not used in tuning process) are compared with metrics from 2 tuned years.

4.3.1 Variance detected in the tuned model

The fraction of observed LSWT variance, var_{min} and var_{max} for non-seasonally ice covered lakes and var_{jas} (K^2) for seasonally ice covered lakes, that is detected in the tuned model, $inter_{min}$, $inter_{max}$, $inter_{jas}$ (R^2_{adj}) is determined as shown in Sect. 2.4.3. The results show that the modelled LSWTs capture less of the true (observed) inter-annual variability in lakes where the observed LSWT variance and the annual LSWT range is low. This indicates that lower latitude lakes and high altitude lakes are less well represented in the model, than lakes with greater observed LSWT variance and the annual range. This would also indicate that Southern hemispheric lakes at 35–55° S are less well represented than lakes in the Northern Hemisphere at the same latitude, as the annual LSWT range is considerably lower at 35–55° S than at 35–55° N (Layden et al., 2015).

For non-seasonally ice covered temperate lakes, the $inter_{max}$ and $inter_{min}$ fraction is substantially greater (0.49 and 0.37) than in tropical lakes (0.07 and 0.13), Table 9. This can be explained by the greater observed variability (var_{max} and var_{min}) in temperate lakes (0.65 and 0.69 K^2), than in tropical lakes (0.12 and 0.15 K^2). Across all non-seasonally ice covered lakes var_{max} and $inter_{max}$ show a correlation of 0.69 and var_{min} and $inter_{min}$ show a correlation of 0.33 ($p < 0.05$), showing that lakes with greater observed variability have a greater portion of the variability detected in the model.

For high altitude seasonally ice covered temperate lakes, the fraction of the observed JAS LSWT inter-annual variability explained by the tuned model is considerably less ($inter_{jas} = 0.21$) than for low altitude lakes (0.52), Table 9. The variability in the observed JAS LSWT for high altitude lakes ($var_{jas} = 0.19$) is almost 4 times lower than for low altitude lakes (0.75). For seasonally ice covered lakes the $inter_{jas}$ and var_{jas} are also correlated, 0.31, $p = 0.000$.

GMDD
8, 8547–8606, 2015

Furthermore, the annual range of monthly LSWTs for non-seasonally ice covered lakes, explain 0.38 and 0.36 ($p = 0.000$) of the variation in $\mathrm{var}_{\mathrm{max}}$ and $\mathrm{var}_{\mathrm{min}}$, with lakes of a low annual range (high altitude and tropical lakes), showing less inter-annual variability. This supports the findings that tropical and high altitude lakes are less well represented in the model.

The relationship between the annual range and $\mathrm{var}_{\mathrm{jas}}$ is not detected in seasonally ice covered lakes. This is most possibly because the inter-lake variance in the annual range of monthly LSWTs is almost 3 times less (22 K^2) than in non-seasonally ice covered lakes (62 K^2). The greater inter-lake variance in the annual monthly LSWTs of non-seasonally ice covered lakes can be attributed to the greater range in latitudes (48° N to 55° S) and the absence of a minimum LSWT restriction due to ice cover.

4.3.2 Comparison of tuned and untuned model LSWTS

The tuning period extends from 8 August 1991 to 31 December 2010. The final year (2011) of available observational ARC-Lake LSWT data is used to independently evaluate the tuning process. The tuned model is forced for the year 2011 and the tuned metrics are quantified. The metrics of this untuned year (2011) are compared with metrics from two tuned years (1996 and 2010), as shown in Tables 10 and 11. The year 1996 is the first full year of data from ATSR2 and 2010 is the last year of tuned data from AATSR.

The mean metric results and the spread of differences across the 135 seasonally ice covered lakes for the tuned and untuned period are highly comparable across all 3 years, showing marginally better MAD metrics for the untuned period. For the 25 shallow lakes tuned with the modified approach, the MAD results for the untuned year are more comparable with 2010 results than the 1996 results.

For the other 3 metrics for the 25 shallow lakes, the untuned year has a lower spread of differences across lakes than for 2010 and a marginally better JAS LSWT and 1 °C cooling day. The spread of differences across lakes for 1 °C warming day for the untuned year is wider than in 2010 but is better than for 1996. The 1 °C cooling and warming day biases for 1996 and 2010 are less comparable for the 25 lakes than for the 135 lakes. This may be because the modelled effect of depth on the metrics are more predictable for deeper lakes, as illustrated in Fig. 16, than for shallow lakes.

Overall, the result of the modelled LSWTs for the untuned year (2011) compare well to the modelled results from the tuned years (1996 and 2010) showing that the model remains stable when run with ERA forcing data outside the tuning period.

For non-seasonally ice covered lakes, the mean MAD and dispersion of errors is slightly higher for the untuned year, 2011, Table 11. However, overall the metrics are very comparable to the metrics from 1996 and 2010.

5 Findings and discussion

5.1 The effect of the 1 °C warming day on JAS LSWT

Through the trial work, the effect of the timing of the 1 °C warming day (indicative of ice-off) on the JAS LSWT and on the timing 1 °C cooling day (indicative of ice-on) of deep high latitude or very deep seasonally ice covered trial lakes is demonstrated. Using the default albedo ($\alpha 1$, Table 2), the modelled 1 °C warming day of the 21 trial lakes occur, on average, 20 days too early. A higher albedo ($\alpha 2$, Table 2) delays the 1 °C warming day by 27 ± 12.6 days and decreases the mean JAS LSWT bias by half, across the 21 lakes. Lake depth and latitude cause much of the modelled inter-lake variability between the length of the delay in the 1 °C warming day and the JAS LSWT decrease. Across the 21 lakes, together (using stepwise regression), they account for 0.50 (R^2_{adj}, $p = 0.001$) of the variance. Separately, depth accounts for 0.35 ($p = 0.003$) and latitude for 0.26 ($p = 0.01$) of the variance. The LSWTs for Great Bear and Great Slave lakes modelled with $\alpha 2$ (high) and $\alpha 1$ (low; default) albedos shown in Fig. 14, clearly show the effect that the later warming day has on the modelled JAS LSWT. Great Slave (62° N and 41 m in depth) and Great Bear (66° N and 72 m in depth), show a JAS LSWT decrease of 4.26 and 3.40 °C as a result of a 28 and 32 day delay in 1 °C warming day. The effect of changes in the 1 °C warming day on the JAS LSWT is only evident in deep lakes; a delay of 29 and 32 days in the 1 °C warming day for Winnebago (44° N) and Khanka (45° N) both with depths of 5 m, resulted in only a small JAS LSWT decrease of ∼ 0.1 °C. The relationship between the JAS LSWT decrease per week of later 1 °C warming day, shown in Fig. 15, demonstrates the greater JAS LSWT change for deeper higher latitude lakes.

This finding is supported by a study on Lake Superior, average depth of 147 m, (Austin and Colman, 2007). A JAS LSWT warming trend (of 2.5 °C from 1979 to 2006) for Lake Superior which is substantially in excess of the air temperature warming trend, was found to be as a result of a longer warming period, caused by an earlier ice-off date of ∼ 0.5 day yr^{-1}.

The modelled results also show that depth explains 0.42 (R^2_{adj}, $p = 0.001$) of the inter-lake variance in the response of the 1 °C cooling day to the decrease in the JAS LSWT. The modelled decrease in the JAS LSWT causes an earlier 1 °C cooling day in deep lakes. For Great Slave (41 m), a decrease of 4.26 °C in the modelled JAS LSWT resulted in an earlier 1 °C cooling day of 3.4 days. The effect is bigger for deeper lakes. For Great Bear (72 m), the JAS LSWT decrease of 3.40 °C causes an earlier 1 °C cooling day of 7.6 days. For the deepest lake in the trials, Lake Hovsgol (138 m) the JAS LSWT decrease of 2.60 °C had the largest effect on 1 °C cooling day, causing it to occur 12.8 days earlier.

The findings are sensible. A delay in the 1 °C warming day, shortening the lake warming period, may not prevent a shallow lake reaching its full heating capacity but may prevent of a deep lake from reaching its maximum heat storage capacity. At higher latitudes, the LSWT warming period for northern hemispheric lakes become increasingly short (Layden et al., 2015). As a result, deep lakes increasingly fall short of reaching their maximum heat storage, causing a greater JAS LSWT decrease. Any changes to the 1 °C warming day of deep and high latitude (or high altitude lakes) will therefore affect JAS LSWT. Deep lakes also cool more slowly than shallow lakes, resulting in a later cooling day.

GMDD
8, 8547–8606, 2015

These findings highlight the sensitivity of the whole LSWT cycle of deep high latitude lakes, to changes in the timing of 1 °C warming day, as illustrated in Fig. 16. This figure also illustrates how an earlier 1 °C cooling day caused by a lower JAS LSWT may be counteracted or masked in deep lakes, where heat is retained during the cooling period.

The effect that depth has on the JAS LSWT is apparent when comparing lakes at the same altitude and latitude but with different depths. For example, Lake Nipigion, located in Canada at 50° N and at 283 m a.s.l., has a mean depth of 55 m and an average JAS LSWT of 4.4 °C lower (15.4 °C) than that of Lake Manitoba (19.8 °C), also located in Canada (at 51° N and 247 m a.s.l.), but with a mean depth of only 12 m.

There is a snow cover module with *FLake* which is not operational in this version of the model, therefore the insulating effect that snow has on the underlying ice is not modelled. As a result the snow and ice albedo are set to the same default value (0.60), possibly underestimating the extent of the albedo effect of snow. This may be the reason for the earlier 1 °C warming day and the higher JAS LSWTs, when modelled with the default albedo. As shown in the tuning process, a higher albedo results in a later (and more timely) 1 °C warming day and as a result, reduces period of time of the surface absorption of short-wave radiation, improving the mean JAS LSWTs.

5.2 Lake bottom temperatures modelled in *FLake*

The month of minimum LSWTs in the annual cycle (monthly minimum) have the potential to be used as a proxy for determining the temperature of the bottom layer (hypolimnion) of non-seasonally ice covered lakes. The monthly minimum climatological ARC-Lake LSWT explains 0.97 (R^2_{adj}) of the variance in the bottom temperatures, obtained from the *FLake* model based on the hydrological year 2005/2006 (Kirillin et al., 2011) and have a 1 : 1 relationship, as shown in Fig. 17. Empirically, it has previously being shown that from the equator to approximately 40° (N/S), the steep decline in the minimum LSWT is reflected in the hypolimnion temperature (Lewis, 1996). The comparability between the monthly minimum LSWT (using the ARC-Lake monthly minimum climatology LSWTs) and the bottom temperature, for all deep (> 25 m) non-seasonally ice covered lakes (14 lakes) supports this empirical observation.

Although, changes in other factors affect hypolimnion temperature, such as influx of cooler water and geothermal heating, the monthly minimum LSWTs from satellite can offer a good indication of hypolimnion temperature in cases where this otherwise can not be or isn't observed directly.

5.3 Wind speed scaling for low latitude lakes

The trials showed that while non-seasonally ice covered lakes at latitudes < 35° N/S required no wind speed scaling (*u1*), non-seasonally ice covered lakes at latitudes > 35° N/S and all seasonally ice covered lakes produced more representative LSWTs using the largest wind speed scaling (*u3*) as outlined in Sect. 2.2.3. For the deep (> 25 m) non-seasonally ice covered lakes (14 lakes), the density difference between the maximum LSWT and the hypolimnion temperature during the stratification period were calculated (Haynes, 2013). The density difference for lakes at latitudes below 35° N/S is substantially lower ($0.352 \times 10\,\mathrm{kg^{-3}\,m^3}$) than for lakes at latitudes above 35° N/S ($1.183 \times 10\,\mathrm{kg^{-3}\,m^3}$).

It is possible that the greater density difference between these two layers (LSWT and hypolimnion) in higher latitude lakes during the stratification period, may produce a stronger buffering effect against wind, than for lakes with a smaller density difference between the two layers.

As winds can drive lake mixing in deep lakes, it strongly influences the epilimnion depth and the LSWT. The larger the density gradient between the maximum LSWT and the hypolimnion during stratification, the more wind energy is required to produce the same amount of mixing than for lakes with a smaller density gradient between the two layers. Although the density differences between the two layers are considered in *FLake*, the wind forcing data purports to U_{land} measurements. It is possible that when forced with an underestimated wind speed, the effect of wind on the LSWT will

GMDD
8, 8547–8606, 2015

be further reduced. As a result, higher latitude lakes may show more representative LSWTs using a higher wind speed scaling.

5.4 Improving modelled LSWTs in *FLake*

The optimal LSWT regulating properties of the 244 lakes provide a guide to improving the LSWT modelling in *FLake* for other lakes, without needing to tune the model.

5.4.1 Depth

The tuning results show that deep lakes are generally tuned to a lower depth and shallower lakes to a greater depth. Figure 18 shows the relationship between the lake-mean depth and the effective (tuned) depth of all 244 successfully tuned lakes, colour coded by the depth factor optimised in the tuning process. The figure legend shows the decrease in the effective depth factor with increasing average lake depth (graphed in the figure insert), providing a means to estimate an appropriate effective depth for any lake with a mean depth from 4–124 m.

The tuned lake depths are sensible. For shallow lakes, tuning to a greater depth may compensate for not having considered the "heat flux from sediments" scheme in the model. The retention of heat in the sediments has the same effect as deepening the lakes, causing an increase the heat storage capacity, which has been demonstrated (Fig. 1b) to reduce the maximum LSWT and delay the 1 °C cooling day.

Many deep lakes have 3 distinct layers, the upper mixed layer (epilimnion), the underlying thermocline (metalimnion) and the bottom layer (hypolimnion). As *Flake* is essentially a two-layer model, it is possible that for deep lakes the mean depth (mean of entire lake depth) is tuned to a shallower depth as it is more representative of the mean depth of the 2 upper lake layers.

Other factors affecting the rate at which heat is exchanged between the atmosphere and the surface water, such as topography, altitude, bathymetry and surface area are not considered in *FLake.* As these factors vary considerably between lakes, it is possible that lake depth tuning may also compensate for the effect that these factors have on the rate of the surface heat exchange.

5.4.2 Light extinction coefficient

Across all lakes, 57 % were tuned to light extinction coefficient values of either κ_{d4} and κ_{d5}. The average depth of lakes tuned to κ_{d4} is 21 and 13 m for lakes tuned to κ_{d5}. Tuning of deeper lakes to the more transparent of these two κ_d values (κ_{d4}) and shallower lakes to the less transparent value (κ_{d5}) makes sense as water clarity of a shallower lake is more affected by the lake bottom sediments than that of deeper lake. In view of this finding and considering that light extinction coefficient values are scare for the majority of lakes, we assess if κ_{d4} and κ_{d5} can be used to provide a good estimation of the light extinction coefficient for modelling LSWTs in *FLake*.

The untuned model is forced using two sets of light extinction coefficient values and the MAD results are compared. In the first model run, the average κ_{sd} (derived from Secchi disk depth data) of the 21 seasonally ice covered trial lakes, 0.82, is applied to all seasonally ice covered lakes and the average k_{sd} of the 14 trial non-seasonally ice covered lakes, 1.46, is applied to all non-seasonally ice covered lakes. In the second run, the model is forced with κ_{d4} applied to all lakes > 16 m in depth and with κ_{d5} for all lakes < 16 m in depth. For both model runs the default albedo and the mean depth are applied and all other model parameters are kept the same. A comparison of the two model runs, show that when LSWTs are modelled with κ_{d4} and κ_{d5} values, the daily MAD is reduced from 3.38 ± 2.74 to $2.28 \pm 2.30\,^{\circ}$C (33 % decrease the average MAD). This indicates that in the absence of available light extinction coefficient values, application of κ_{d4} and κ_{d5} values improve the modelling of LSWTs of large lakes in *FLake*.

5.4.3 Albedo

For seasonally ice covered lakes, only 19 % of the lakes were tuned to the default albedo, $\alpha 1$, (snow and white ice = 0.60 and melting snow and blue ice = 0.10). 64 % of lakes were tuned to two higher albedos $\alpha 2$ or $\alpha 3$, (snow and white ice = 0.80 and melting snow and blue ice = 0.60 for $\alpha 2$ or 0.40 for $\alpha 3$), indicating that the default albedo is too low. To obtain a more timely (later) ice-off and to help address the over-estimated JAS LSWTs, the albedo value $\alpha 3$ (snow and white ice = 0.80, melting snow and blue ice = 0.40) is recommended in place default value ($\alpha 1$). The $\alpha 3$ values are highly comparable to albedo values measured on a Lake in Minnesota using radiation sensors, where the mean albedo of new snow was shown to be 0.83 and the mean ice albedo (after snow melt) was 0.38 (Henneman and Stefan, 1999).

6 Summary and conclusions

The 1-dimensional freshwater lake model, *FLake*, was successfully tuned for 244 globally distributed large lakes using observed LSWTs (ARC-Lake), for the period 1991 to 2010. This process substantially improves the measured biases in various features of the lake annual cycle (including saline and high altitude lakes), as summarised in Table 5 using only 3 lake properties (depth, snow and ice albedo and light extinction co-efficient).

In the process of tuning the model, we demonstrate several aspects of LSWT behaviour, in a way that cannot be done using the LSWT observations alone. We demonstrate the dependency of the whole modelled LSWT cycle of deep high latitude or high altitude lakes, on changes in the timing of the 1 °C warming day (indicative of ice-off). The monthly minimum LSWTs from satellite are demonstrated to offer a good indication of the modelled lake bottom temperature (1 : 1), Fig. 17. This is highly useful where lake bottom temperatures can not be or isn't observed directly.

By determining the amount of observed LSWT variance detected in the tuned model, it can be concluded that lower latitude and high altitude lakes (lakes where the observed LSWT variance and annual range is low) are less well represented in the model, than lakes with greater observed LSWT variance and the annual range.

We found that wind speed with no scaling, *u1*, is most appropriate for lakes at lower latitudes, $< 35°$ N/S, and that wind speed with the largest scaling (*u3*; $U_{\text{water}} = 1.62 + 1.17U_{\text{land}}$), is most appropriate for lakes at higher latitudes $> 35°$ N/S. A greater wind speed scaling for high latitude lakes may be required to overcome a greater buffering effect possibly caused by a greater temperature and density difference between the maximum LSWT and the hypolimnion during stratification than in low latitude lakes.

The optimal LSWT regulating properties of the 244 lakes are shown to be sensible and provide a guide to improving the LSWT modelling in *FLake* for other lakes, without having to tune the model.

The relationship between the lake-mean depth and the effective (tuned) depth of all 244 successfully tuned lakes, show that deep lakes are generally tuned to a lower depth and shallower lakes to a greater depth. Figure 18, provides a means to estimate an appropriate effective depth for any lake with a mean depth from 4–124 m. An albedo value $\alpha 3$ (snow and white ice = 0.80, melting snow and blue ice = 0.40) is recommended in place default value ($\alpha 1$).

Where κ values are unknown, applying κ_{d4} for lakes > 16 m in depth and κ_{d5} for lakes < 16 m in depth improves the modelled LSWT.

This paper predominantly focused on the tuning of *FLake* and interpretation of the LSWT annual cycle using the tuned model. The tuned model forced with ERA data over the available time span of LSWT observations (16–20 years), has the potential to be forced with the complete time span of available ERA data, available for a period of > 33 years; 1979–2012. This offers the potential to provide a better representation of LSWTs changes over a longer period of time, as satellite observations for the relatively short period may reflect some inter-annual variability rather the true changes. As demonstrated, the use of remote sensing and modelled LSWTs together extend the reliable quantitative details of lake behaviour beyond the information from either remote sensing or models alone. The ARC-Lake dataset has since been extended to include ∼ 1000 smaller lakes (surface area > 100 km^2) worldwide, offering the potential to further quantity aspects of lake behaviour worldwide.

Code availability

The code for the *FLake* model can be obtained from the following website; http://www.flake.igb-berlin.de/sourcecodes.shtml

Current Code Owner: DWD, Dmitrii Mironov

Phone: +49-69-8062 2705

Fax: +49-69-8062 3721

E-mail: dmitrii.mironov@dwd.de

History

Version: 1.00 Date: 17 November 2005

Modification comments:

In the MODULE flake_parameters where the values of empirical constants of the lake model *FLake* and of several thermodynamic parameters are set, the "temperature of maximum density of fresh water", tpl_T_r, = 277.13 K (3.98 °C).

In the SUBROUTINE flake_driver (flake_driver.incf), the model uses a number of algorithms to update the bottom temperature, for example its relationship with mixed layer depth. As *FLake* is intended for cold water lakes, if the bottom temperature shows no relationship with the mixed layer depth, the models sets the lake bottom temperature to the temperatures of maximum density (3.98 °C). This creates a problem when modelling tropical lakes; it causes the model to spin up to a wrong "attracter". This problem manifested itself in both the temperature profile and the mixed layer depth.

To overcome this problem, the lake bottom temperature for non-seasonally ice covered lakes in August; tropical winter, was used to set to the temperature of maximum density, before compiling and running the model.

Language: Fortran 90.

Software Standards: “European Standards for Writing and Documenting Exchangeable Fortran 90 Code”.

The Supplement related to this article is available online at doi:10.5194/gmdd-8-8547-2015-supplement.

Author contributions. A. Layden developed and applied the tuning methodology and code, accessed all meteorological and LSWT data, performed the data analysis and prepared the manuscript. S. MacCallum derived the ARC-Lake LSWT observations and provided technical support. C. Merchant initiated the ARC-Lake project and supervised the work in this study.

Acknowledgements. The authors gratefully acknowledge that this work is funded by the European Space Agency under contract 22184/09/I-OL.

The authors also gratefully acknowledge Georgy Kirillin, the author of *FLake* lake model.

References

Armengol, J., Caputo, L., Comerma, M., Feijoó, C., García, J. C., Marcé, R., Navarro, E., and Ordoñez, J.: Sau reservoir's light climate: relationships between Secchi depth and light extinction coefficient, Limnetica, 22, 195–210, 2003.

Ashton, G. D.: River and Lake Ice Engineering, Water Resources Publication, Littleton, CO, 355 pp., 1986.

Austin, J. A. and Colman, S. M.: Lake Superior summer water temperatures are increasing more rapidly than regional air temperatures: a positive ice-albedo feedback, Geophys. Res. Lett., 34, L06604, doi:10.1029/2006GL029021, 2007.

Bernhardt, J., Engelhardt, C., Kirillin, G., and Matschullat, J.: Lake ice phenology in Berlin-Brandenburg from 1947–2007: observations and model hindcasts, Climatic Change, 112, 791–817, 2012.

Brown, L. C. and Duguay, C. R.: The response and role of ice cover in lake-climate interactions, Prog. Phys. Geog., 34, 671–704, doi:10.1177/0309133310375653, 2010.

Bukata, R. P., Jerome, J. H., and Bruton, J. E.: Relationships among secchi disk depth, beam attenuation coefficient, and irradiance attenuation coefficient for great-lakes waters, J. Gt. Lakes Res., 14, 347–355, doi:10.1016/S0380-1330(88)71564-6, 1988.

Dee, D. P., Uppala, S. M., Simmons, A. J., et al.: The ERA-Interim reanalysis: configuration and performance of the data assimilation system, Q. J. Roy. Meteor. Soc., 137, 553–597, doi:10.1002/qj.828, 2011.

Dutra, E., Stepanenko, V. M., Balsamo, G., Viterbo, P., Miranda, P. M. A., Mironov, D., and Schaer, C.: An offline study of the impact of lakes on the performance of the ECMWF surface scheme, Boreal Environ. Res., 15, 100–112, 2010.

ECMWF: European Centre for Medium-Range Weather Forecasts. ECMWF ERA-Interim Re-Analysis data, [Internet], NCAS British Atmospheric Data Centre, September 2009–November 2012, available at: http://badc.nerc.ac.uk/view/badc.nerc.ac.uk__ATOM__dataent_12458543158227759 (last access: November 2012), 2009.

Haynes, W. M.: CRC Handbook of Chemistry and Physics, 94th Edn., Taylor & Francis Limited, Florida, USA, 2013.

Henneman, H. E. and Stefan, H. G.: Albedo models for snow and ice on a freshwater lake, Cold Reg. Sci. Technol., 29, 31–48, 1999.

Herdendorf, C. E.: Large Lakes of the World, J. Gt. Lakes Res., 8, 379–412, 1982.

Holmes, R. W.: Secchi disk in turbid coastal waters, Limnol. Oceanogr., 15, 688–694, 1970.

Hsu, S. A.: Coastal Meteorology, Academic Press Inc., San Diego, USA, 1988.

ILEC: World Lake Database, International Lake Environment Committee Foundation, available at: http://wldb.ilec.or.jp (last access: May 2011), 1999.

Jerlov, N. G.: Marine Optics, Elsevier Scientific Publishing Company, Amsterdam, the Netherlands, 1976.

Kirillin, G., Hochschild, J., Mironov, D., Terzhevik, A., Golosov, S., and Nutzmann, G.: *FLake*-Global: online lake model with worldwide coverage, Environ. Modell. Softw., 26, 683–684, 2011.

Kourzeneva, E., Asensio, H., Martin, E., and Faroux, S.: Global gridded dataset of lake coverage and lake depth for use in numerical weather prediction and climate modelling, Tellus A, 64, 15640, doi:10.3402/tellusa.v64i0.15640, 2012.

LakeNet: LakeNet's Global Lake Database, available at: http://www.worldlakes.org (last access: May 2011), 2003.

Launiainen, J. and Cheng, B.: Modelling of ice thermodynamics in natural water bodies, Cold Reg. Sci. Technol., 27, 153–178, 1998.
Layden, A., Merchant, C. and MacCallum, S.: Global climatology of surface water temperatures of large lakes by remote sensing, Int. J. Climatol., doi:10.1002/joc.4299, online first, 2015.
Lehner, B. and Doll, P.: Development and validation of a global database of lakes, reservoirs and wetlands, J. Hydrol., 296, 1–22, doi:10.1016/j.jhydrol.2004.03.028, 2004.
Lerman, A., Imboden, D., and Gat, J.: Physics and Chemistry of Lakes, Verlag Springer, Berlin, Heidelberg, 1995.
Lewis Jr., W. M.: Tropical lakes: how latitude makes a difference, in: Perspectives in Tropical Limnology, edited by: Schiemer, F. and Boland, K. T., SPB Academic Publishers, Amsterdam, the Netherlands, 43–64, 1996.
Long, Z., Perrie, W., Gyakum, J., Caya, D., and Laprise, R.: Northern lake impacts on local seasonal climate, J. Hydrometeorol., 8, 881–896, 2007.
MacCallum, S. N. and Merchant, C. J.: Surface water temperature observations of large lakes by optimal estimation, Candian Journal of Remote Sensing, 38, 25–45, doi:10.5589/m12-010, 2012.
Mironow, D. V.: Parameterization of lakes in numerical weather prediction, description of a lake model, German Weather Service, Offenbach am Main, Germany, 2008.
Monson, B.: A Primer on Limnology, Water Resources Center, University of Minnesota, St Paul, MN, 1992.
Poole, H. H. and Atkins, W. R. G.: Photo-electric measurements of submarine illumination throughout the year, Jour Marine Biol Assoc United Kingdom, 16, 297–324, 1929.
Pour, H. K., Duguay, C. R., Martynov, A., and Brown, L. C.: Simulation of surface temperature and ice cover of large northern lakes with 1-D models: a comparison with MODIS satellite data and in situ measurements, Tellus A, 64, 17614, doi:10.3402/tellusa.v3464i3400.17614, 2012.
Resio, D. T., Bratos, S. M., and Thompson, E. F.: Meteorology and Wave climate, in: Coastal Engineering Manual, chapter II-2. U.S. Army Corps of Engineers. Washington, DC, USA, 2003.
Sherwood, I.: On the Universality of the Poole and Atkins Secchi Disk-light Extinction Equation, U.S. Water Conservation Lab, Phoenix, Arizona 85040, USA, 1974.
Voros, M., Istvanovics, V., and Weidinger, T.: Applicability of the *FLake* model to Lake Balaton, Boreal Environ. Res., 15, 245–254, 2010.

Table 1. ERA data components and description and *Flake* input format.

ERA data components and description	*Flake* input
SSRD; 3 hourly shortwave solar downward radiation, cumulative over 12 h forecasts ($W m^{-2}$)	Mean daily SSRD $W m^{-2}$
T2; 6 hourly air temperature at 2 m (K)	Mean daily T2 (°C)
D2; 6 hourly dewpoint at 2 m (K),	Mean daily vapour pressure (hPa) $= P(z) \times 10^{(7.5(\text{dewpoint}/(237.7+\text{dewpoint})))}$ Where $P(z) = P(\text{sea level}) \times \exp(-z/H)$. $P(z)$ = pressure at height z, P(sea level) = sea level pressure (∼ 1013 mb), z = height in metres, H = scale height (∼ 7 km) http://www.reahvac.com/tools/humidity-formulas/
U10 and V10; 6 hourly wind components at 10 m ($m s^{-1}$)	Mean daily wind speed ($m s^{-1}$); $= \text{sqrt}(V10^2 + U10^2)$
TCC; 6 hourly total cloud cover	Mean daily TCC

GMDD
8, 8547–8606, 2015

Title Page
Abstract Introduction
Conclusions References
Tables Figures
Back Close
Full Screen / Esc
Printer-friendly Version
Interactive Discussion

Table 2. Lake depth, light extinction coefficient and albedo factor/values used in tuning study; 80 possible combinations for seasonally ice covered lakes (plain text only) and 60 possible combinations for non-seasonally ice covered lakes (plain and bold text; all 6 Z_d factors × all 10 κ_d values).

Lake depth Z_d	Light extinction coefficient				albedo α	Snow and white ice Albedo	Melting snow and blue ice albedo
	κ_d	375 nm	475 nm	700 nm			
Z_{d1}	κ_{d1}	0.038	0.018	0.56	$\alpha 1$	0.60	0.10
	$\boldsymbol{\kappa_{d2}}$	**0.052**	**0.025**	**0.57**	$\alpha 2$	0.80	0.60
Z_{d2} (Z_{d1} × 0.75)	κ_{d3}	0.066	0.033	0.58	$\alpha 3$	0.80	0.40
Z_{d3} (Z_{d1} × 0.50)	$\boldsymbol{\kappa_{d4}}$	**0.122**	**0.062**	**0.61**	$\alpha 4$	0.60	0.30
Z_{d4} (Z_{d1} × 1.50)	κ_{d5}	0.22	0.116	0.66			
	κ_{d6}	0.80	0.17	0.65			
$\boldsymbol{Z_{d5}}$ **($\boldsymbol{Z_{d1}}$ × 0.30)**	$\boldsymbol{\kappa_{d7}}$	**1.10**	**0.29**	**0.71**			
$\boldsymbol{Z_{d6}}$ **($\boldsymbol{Z_{d1}}$ × 2.50)**	κ_{d8}	1.60	0.43	0.80			
	κ_{d9}	2.10	0.71	0.92			
	$\boldsymbol{\kappa_{d10}}$	**3.00**	**1.23**	**1.10**			

GMDD
8, 8547–8606, 2015

Table 3. Relationship between the LSWT regulating properties and primary metrics, showing the equations for determining MAD and the JAS LSWT bias.

LSWT regulating properties	Effect on metric	Metrics
κ	κ affects irradiance transmission of surface water, which is more notable in summer months.	Mean JAS LSWT bias (°C) $= \left(\bar{x}_i^{\text{mod\_jas}} - \bar{x}_i^{\text{obs\_jas}}\right)$ $^{\text{mod\_jas}}$ = modelled JAS LSWT $^{\text{obs\_jas}}$ = observed JAS LSWT
d	d alters heat storage capacity affecting timing of the start of the cold phase (the day that the LSWT drops to below 1 °C)	1 °C cooling day bias (days)
α	α alters ice/snow reflectance affecting the end of the cold phase (the day that the LSWT increases to above 1 °C)	1 °C warming day bias (days)
d, α and κ	All LSWT regulating properties contribute to the comparability of the modelled and observed LSWT	Daily MAD (°C) $= \sum \left(\text{abs}\left(x_i^{\text{mod}} - x_i^{\text{obs}}\right)\right)/N;$ $^{\text{mod}}$ = daily modelled LSWTs $^{\text{obs}}$ = daily observed LSWTs N = sample size

GMDD
8, 8547–8606, 2015

Table 4. The effect of wind speed scalings on untuned modelled LSWTs of the seasonally and non-seasonally ice covered trial lakes, with the spread of differences across lakes, 2σ. Results highlight that *u3* is most applicable to seasonally ice covered lakes but there is no one wind speed most suited for all lakes (While the average bias is improved with *u3*, the spread of biases across lakes for mth_{min} and mth_{max} show little change).

Trial results for untuned model							
Seasonally ice covered trial lakes (21 lakes)				Non-seasonally ice covered lakes (14 lakes)			
Metrics	*u1*	*u2*	*u3*	Metric	*u1*	*u2*	*u3*
MAD (°C)	3.07 ±2.25	2.66 ±1.93	2.02 ±1.30	MAD (°C)	3.55 ±3.20	3.11 ±2.77	2.17 ±1.93
Mean JAS bias (°C)	3.71 ±3.51	3.07 ±3.41	1.87 ±2.93	mth_{max} (°C)	1.92 ±5.05	1.39 ±5.06	−0.42 ±5.18
1 °C cooling day bias (days)	12.0 ±39.6	7.9 ±33.3	1.0 ±30.5	mth_{min} (°C)	3.71 ±4.33	3.08 ±4.16	1.47 ±3.87
1 °C warming day Bias (days)	−27.1 ±29.7	−23.6 ±22.7	−20.3 ±18.4				

GMDD
8, 8547–8606, 2015

Determining LSWTs worldwide

A. Layden et al.

Table 5. Summary of the untuned and tuned metrics for the trial seasonally and non-seasonally ice covered lakes and the tuned metrics for all seasonally and non-seasonally ice covered lakes showing the spread of differences across lakes, 2σ.

Seasonally ice covered lakes				Non-seasonally ice covered lakes			
Metrics	Untuned (21 trial lakes)	Tuned (21 trial lakes)	Tuned (160 lakes)	Metrics	Untuned (14 trial lakes)	Tuned (14 trial lakes)	Tuned (84 lakes)
MAD (°C)	3.07 ±2.25	0.84 ±0.51	0.80 ±0.56	MAD (°C)	3.55 ±3.20	0.96 ±0.63	0.96 ±0.66
Mean JAS LSWT bias (°C)	3.71 ±3.51	−0.12 ±1.09	−0.06 ±1.15	mth_{max} (°C)	1.92 ±5.05	−0.44 ±1.52	−0.21 ±1.47
1 °C cooling day bias (days)	12.0 ±39.6	−1.6 ±12.8	−1.08 ±8.5	mth_{min} (°C)	3.71 ±4.33	−0.03 ±1.48	−0.08 ±1.47
1 °C warming day bias (days)	- 27.1 ±29.7	−0.2 ±10.7	0.3 ±12.3				

GMDD
8, 8547–8606, 2015

Table 6. Metric results for seasonally ice-covered lakes (135 lakes using the original tuned set-up, Table 2 and 25 lakes tuned with the modified set-up), compared with the results for the trial lakes, showing the spread of differences across lakes, 2σ.

Tuning metrics	135 lakes	25 lakes (modified set-up)	All lakes (160)	Trial lakes
MAD (°C)	0.74 ± 0.48	1.11 ± 0.56	0.80 ± 0.56	0.84 ± 0.51
Mean JAS bias (°C)	-0.01 ± 1.11	-0.34 ± 1.22	-0.06 ± 1.15	-0.12 ± 1.09
1 °C cooling day bias (days)	-1.0 ± 8.8	-1.3 ± 6.9	-1.08 ± 8.5	-1.6 ± 12.8
1 °C warming day Bias (days)	0.5 ± 12.6	-0.5 ± 10.2	0.3 ± 12.3	-0.2 ± 10.7

GMDD
8, 8547–8606, 2015

GMDD
8, 8547–8606, 2015

Determining LSWTs worldwide

A. Layden et al.

Table 7. Comparison of tuned model results for saline, freshwater, high and low altitude seasonally ice covered lakes, with the spread of differences across lakes, 2σ.

Tuned metrics	Tuned results for 160 seasonally ice covered lakes			
	Saline (37 lakes)	Freshwater (123 lakes)	Altitude > 3200 m a.s.l. (14 lakes)	Altitude < 2000 m a.s.l. (146 lakes)
MAD (°C)	0.90 ± 0.69	0.76 ± 0.50	0.61 ± 0.24	0.81 ± 0.57
Mean JAS bias (°C)	-0.23 ± 1.14	-0.01 ± 1.14	0.06 ± 1.14	-0.07 ± 1.15
1 °C cooling day bias (days)	-1.3 ± 9.7	-1.0 ± 8.3	-3.1 ± 10.8	-0.9 ± 8.2
1 °C warming day Bias (days)	0.0 ± 13.1	0.4 ± 12.0	0.9 ± 13.6	0.3 ± 12.1

Table 8. Comparison of tuned metric results for saline, freshwater and high and low altitude non-seasonally ice covered lakes, with the spread of differences across lakes, 2σ.

Tuned metrics	Tuned results for 84 non-seasonally ice covered lakes			
	Saline (26 lakes)	Freshwater (58 lakes)	Altitude > 1500 m a.s.l. (10 lakes)	Altitude < 1500 m a.s.l. (74 lakes)
MAD (°C)	1.06 ± 0.67	0.91 ± 0.64	1.03 ± 0.82	0.95 ± 0.64
mth_{max} (°C)	-0.31 ± 1.90	-0.16 ± 1.24	-0.40 ± 2.12	-0.18 ± 1.37
mth_{min} (°C)	-0.25 ± 1.74	-0.01 ± 1.33	-0.14 ± 1.30	-0.07 ± 1.50

Discussion Paper | Discussion Paper | Discussion Paper | Discussion Paper |

GMDD

8, 8547–8606, 2015

Determining LSWTs worldwide

A. Layden et al.

Table 9. The fraction (R^2_{adj}) of observed inter-annual variability detected in the model, for the maximum and minimum LSWT for non-seasonally ice covered lakes ($inter_{max}$ and $inter_{min}$) and for the JAS LSWT for seasonally ice covered lakes, ($inter_{jas}$), highlighting that where the observed inter-annual variability is low, the proportion of variability detected in the model is also low (high altitude seasonally ice covered lakes and tropical lakes).

Non-seasonally ice covered lakes	All lakes (84)	Temperate lakes > 20° N/S (44 lakes)	Tropical lakes < 20° N/S (40 lakes)
$inter_{max}$ (R^2_{adj})	0.29 ± 0.63	0.49 ± 0.58	0.07 ± 0.31
$inter_{min}$ (R^2_{adj})	0.25 ± 0.49	0.37 ± 0.49	0.13 ± 0.37
var_{max} (K^2)	0.40	0.65	0.12
var_{min} (K^2)	0.43	0.69	0.15
Seasonally ice covered lakes	**All lakes (160)**	**Altitude > 3200 m a.s.l. (14 lakes)**	**Altitude < 2000 m a.s.l. (146 lakes)**
$Inter_{jas}$ (R^2_{adj})	0.50 ± 0.62	0.21 ± 0.46	0.52 ± 0.59
var_{jas} (K^2)	0.70	0.19	0.75

GMDD
8, 8547–8606, 2015

Table 10. Results of independent evaluation of the tuning process for seasonally ice covered lakes with the spread of differences across lakes, 2σ, showing that the metrics from the untuned year (2011) compare well with metrics from 1996 (the first full year of data from ATSR2) and 2010 (the last year of tuned data from AATSR).

Tuned metrics	135 lakes			25 lakes (modified set-up)		
	2011 Untuned	1996 Tuned (ATSR2)	2010 Tuned (AATSR)	2011 Untuned	1996 Tuned (ATSR2)	2010 Tuned (AATSR)
MAD (°C)	0.86 ± 0.68	0.89 ± 0.74	0.87 ± 0.71	1.59 ± 1.04	1.33 ± 0.79	1.66 ± 0.95
Mean JAS bias (°C)	0.18 ± 1.50	−0.33 ± 1.79	0.28 ± 1.44	0.12 ± 1.71	0.17 ± 1.19	0.28 ± 1.81
1 °C cooling day bias (days)	11.1 ± 23.8	5.1 ± 25.6	8.5 ± 21.4	10.9 ± 18.7	−3.0 ± 41.9	11.7 ± 31.3
1 °C warming day bias (days)	7.4 ± 19.7	12.1 ± 19.7	6.5 ± 19.8	9.33 ± 21.6	13.2 ± 18.2	1.0 ± 32.54

GMDD
8, 8547–8606, 2015

Determining LSWTs worldwide

A. Layden et al.

Table 11. Results of the independent evaluation of the tuning process for non-seasonally ice covered lakes 3 with the spread of differences across lakes, 2σ, showing the untuned year (2011) with the first full year of data from ATSR2 (1996) and the last year of tuned data from AATSR (2010).

Tuned Metrics	2011 Untuned	1996 Tuned (ATSR2)	2010 Tuned (AATSR)
MAD (°C)	1.07 ± 0.91	0.98 ± 0.82	0.97 ± 0.81
mth_{max} (°C)	-0.23 ± 2.40	-0.32 ± 1.86	-0.31 ± 2.20
mth_{min} (°C)	-0.02 ± 2.04	-0.23 ± 1.73	$+0.11 + 2.15$

GMDD
8, 8547–8606, 2015

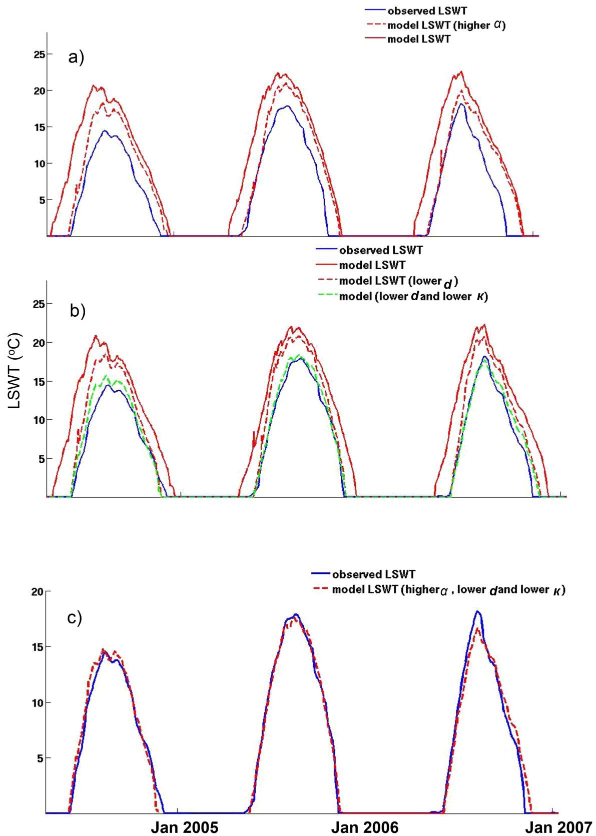

Figure 1. Preliminary modelled runs for Lake Athabasca showing that adjustments to d, α and κ can greatly improve the modelled LSWTs compared to the default/recommended d, α and κ values; **(a)** shows that a higher α causes a later and more timely ice-off date **(b)** shows that a lower d causes an earlier and more timely ice-on date and a lower κ value (greater transparency) reduces the maximum LSWT and **(c)** shows that the combined effect of the adjusted d, α and κ produce LSWTs that are highly comparable to the observed LSWTs.

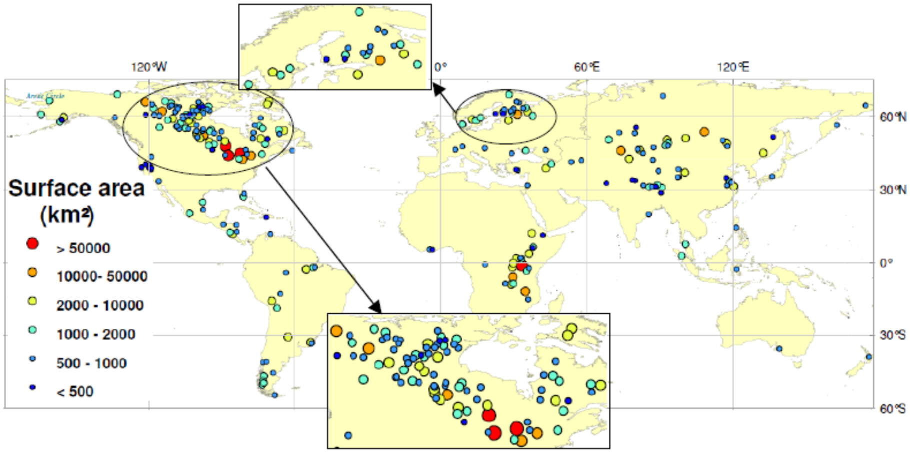

Figure 2. Location of 246 observed lakes colour coded by surface area (obtained using polygon area in GLWD) showing zoomed inset of North America and Northern Europe.

GMDD
8, 8547–8606, 2015

Determining LSWTs worldwide

A. Layden et al.

Title Page
Abstract Introduction
Conclusions References
Tables Figures
Back Close
Full Screen / Esc
Printer-friendly Version
Interactive Discussion

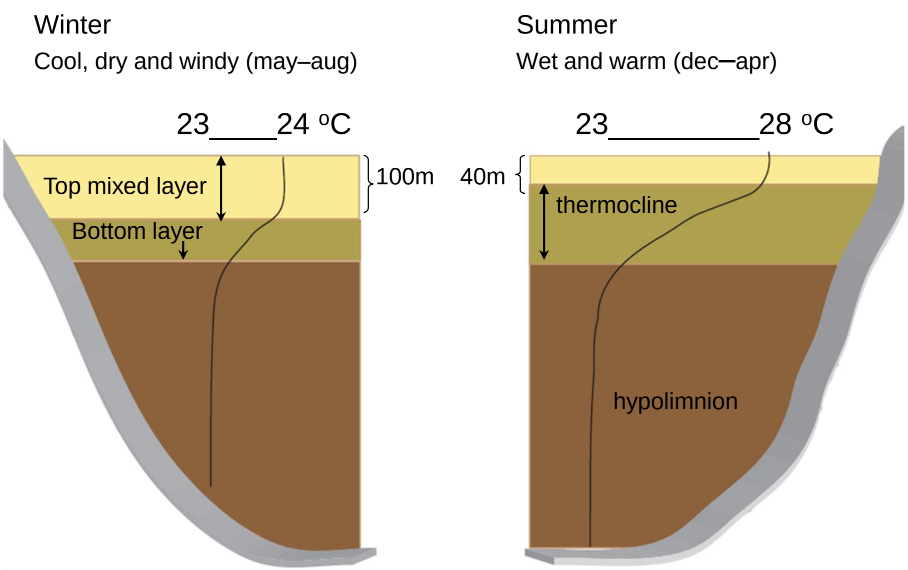

Figure 3. Summer and winter mixing and temperature profile of Lake Malawi; showing a mixed layer depth of 40–100 m. FLake predicts the LSWT and depth of the "upper mixed layer" and the temperature of the "bottom layer".

GMDD
8, 8547–8606, 2015

Determining LSWTs worldwide

A. Layden et al.

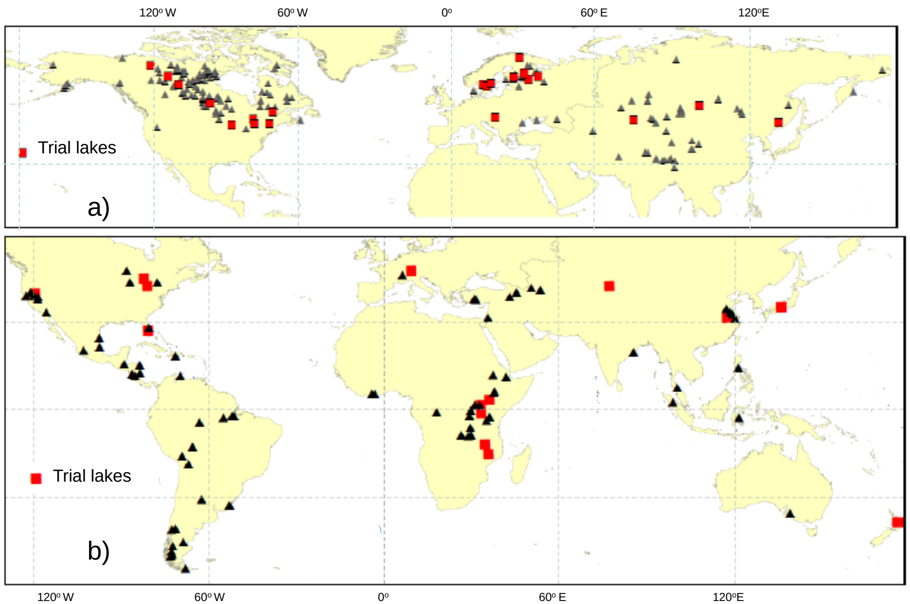

Figure 4. Location of lakes, with red square showing the trial lakes **(a)** 160 seasonally ice covered lakes, including 21 trial lakes and **(b)** 86 non-seasonally ice covered lakes including 14 trial lakes.

GMDD
8, 8547–8606, 2015

Determining LSWTs worldwide

A. Layden et al.

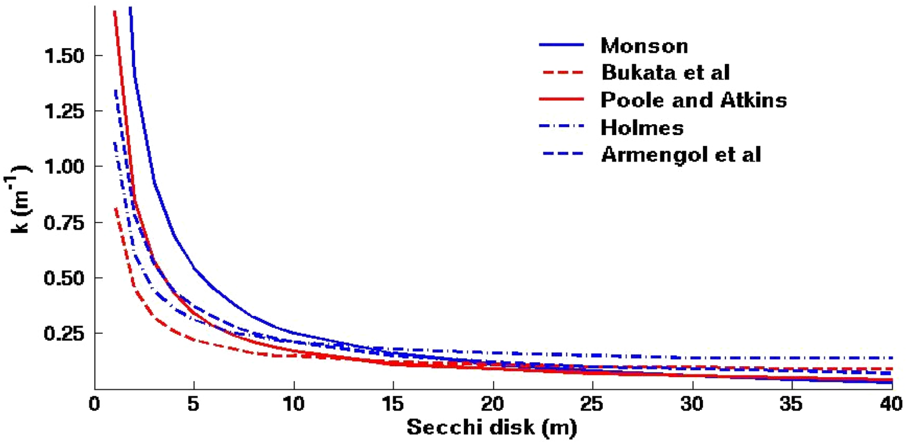

Figure 5. A comparison of 5 methods relating light extinction coefficients to Secchi disk depths, showing that all method compare well at Secchi disk depths > 10 m.

GMDD
8, 8547–8606, 2015
Determining LSWTs worldwide
A. Layden et al.

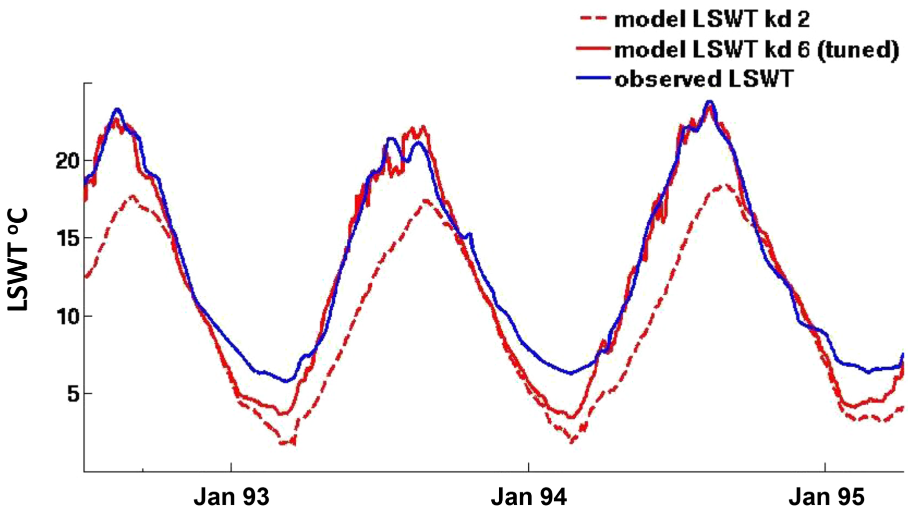

Figure 6. LSWTs for Lake Geneva modelled with two different κ_d values ($\kappa_{d2}\kappa_{d6}$) shows the substantially stronger effect of κ_d on the maximum LSWT than the minimum LSWT.

GMDD
8, 8547–8606, 2015

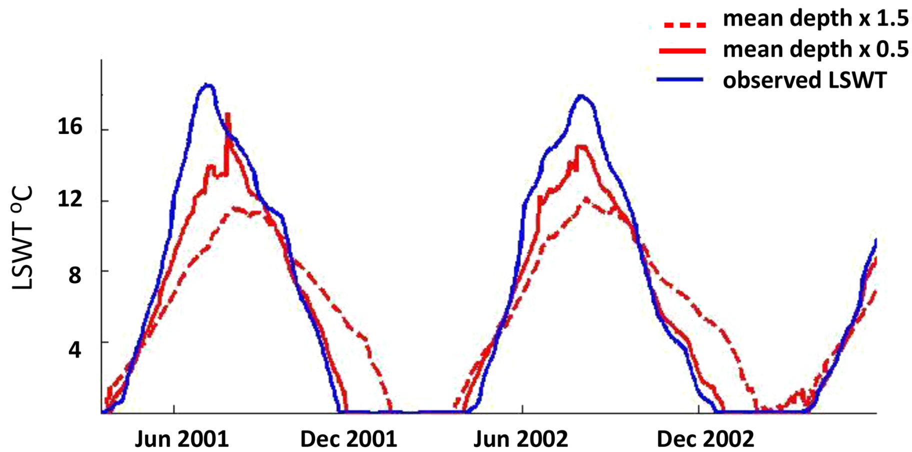

Figure 7. Effect of depth on LSWT for Lake Ladoga, Russia (mean depth 52 m), showing that when modelled with a greater depth, the lake cools later and the maximum LSWT is lower.

GMDD
8, 8547–8606, 2015

Determining LSWTs worldwide

A. Layden et al.

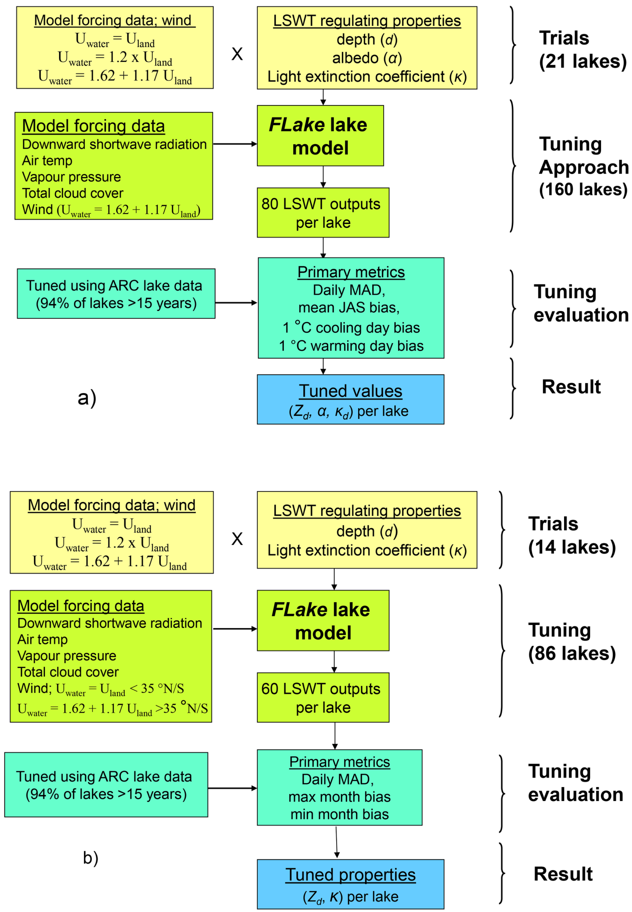

Figure 8. Tuning approach overview for **(a)** seasonally ice covered lakes and **(b)** non-seasonally ice covered lakes.

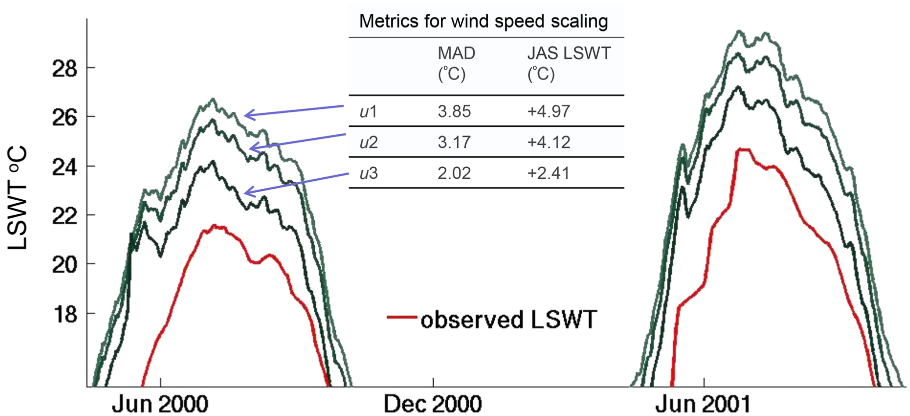

Figure 9. Effect of wind speed scalings on modelled LSWT for Lake Simcoe, Canada, showing that the *u3* scaling halves the daily MAD and JAS LSWT bias.

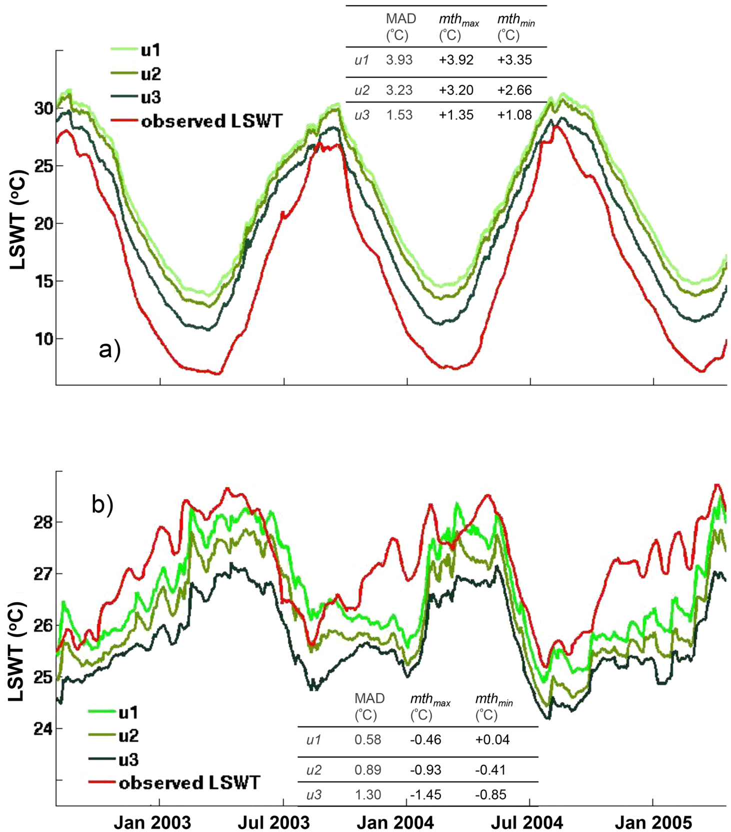

Figure 10. Effect of wind speed scaling on LSWT for a temperate non-seasonally ice covered lake **(a)** Lake Biwa, Japan (35.6° N) and for a tropical non-seasonally ice covered lake **(b)** Lake Turkana, Africa (3.5° N) showing that the modelled LSWT for the temperate lake is better represented using *u3* and the modelled LSWT for the tropical lake is better represented using *u1*.

GMDD
8, 8547–8606, 2015

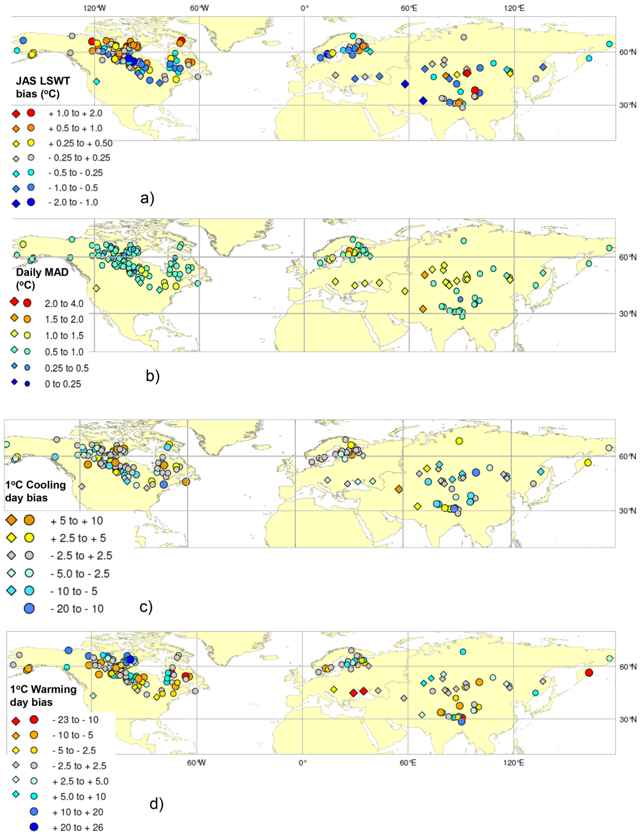

Figure 11. Tuning metric results for all 160 lakes with seasonal ice cover. The results for the 25 lakes tuned with modified are marked by diamond symbols **(a)** JAS bias, **(b)** MAD bias, **(c)** 1 °C cooling day bias and **(d)** 1 °C warming day bias.

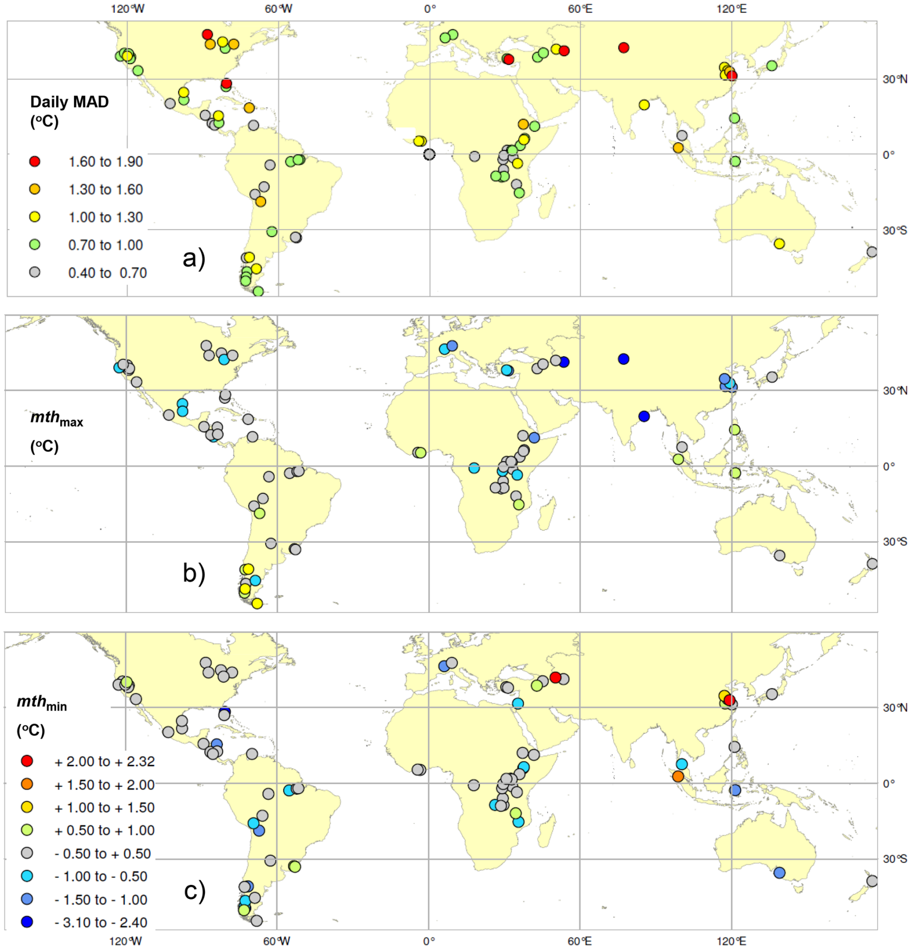

Figure 12. Tuning metric results for the 84 lakes with non-seasonally ice cover lakes **(a)** MAD, **(b)** mth_{max} and **(c)** mth_{min}.

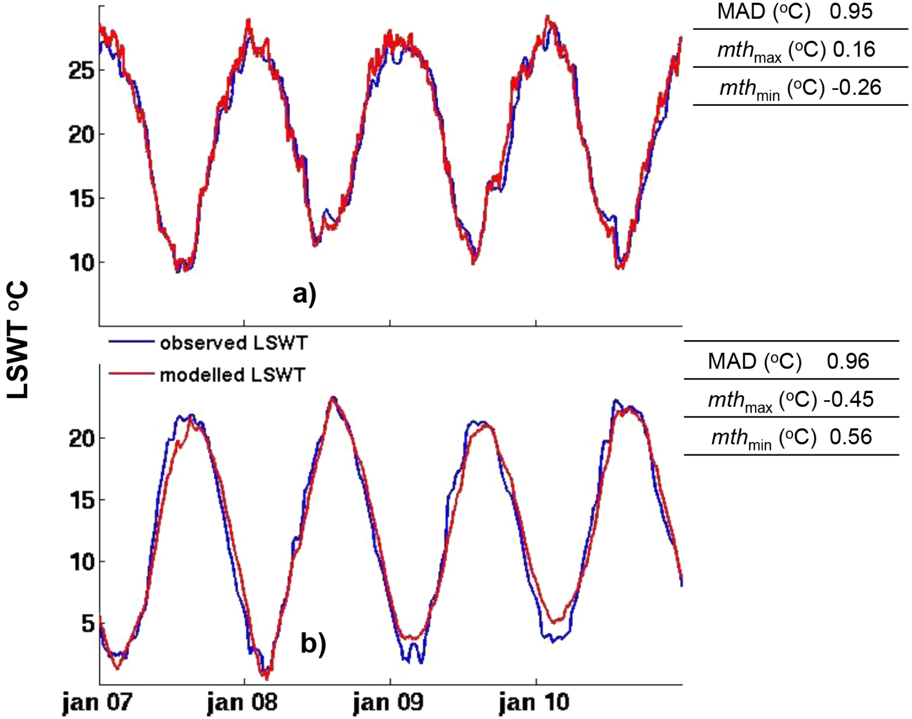

Figure 13. Observed LSWT vs. tuned model LSWT for saline and high altitude lakes **(a)** Lake Chiquita, Argentina (31° S, salinity 145 $g L^{-1}$) **(b)** Lake Van, Turkey (38° N, 1638 m a.s.l., salinity 22 $g L^{-1}$).

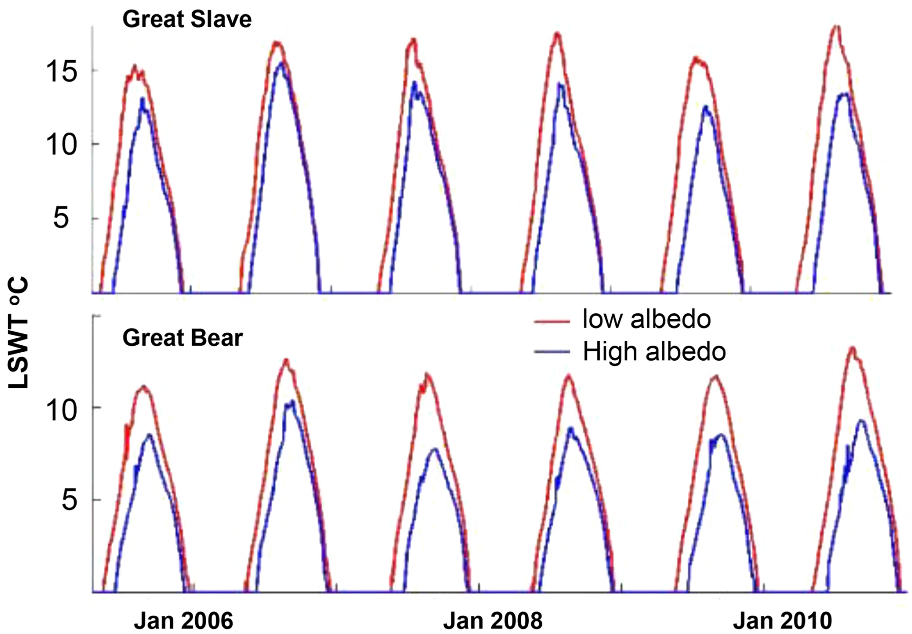

Figure 14. LSWTS for Great Bear and Great Slave modelled with low albedo (default albedo) and high albedo (snow and white ice = 0.80 and melting snow and blue ice = 0.60) demonstrating that the higher albedo delays the 1 °C warming day, causing a lower JAS LSWT.

GMDD
8, 8547–8606, 2015

Determining LSWTs worldwide

A. Layden et al.

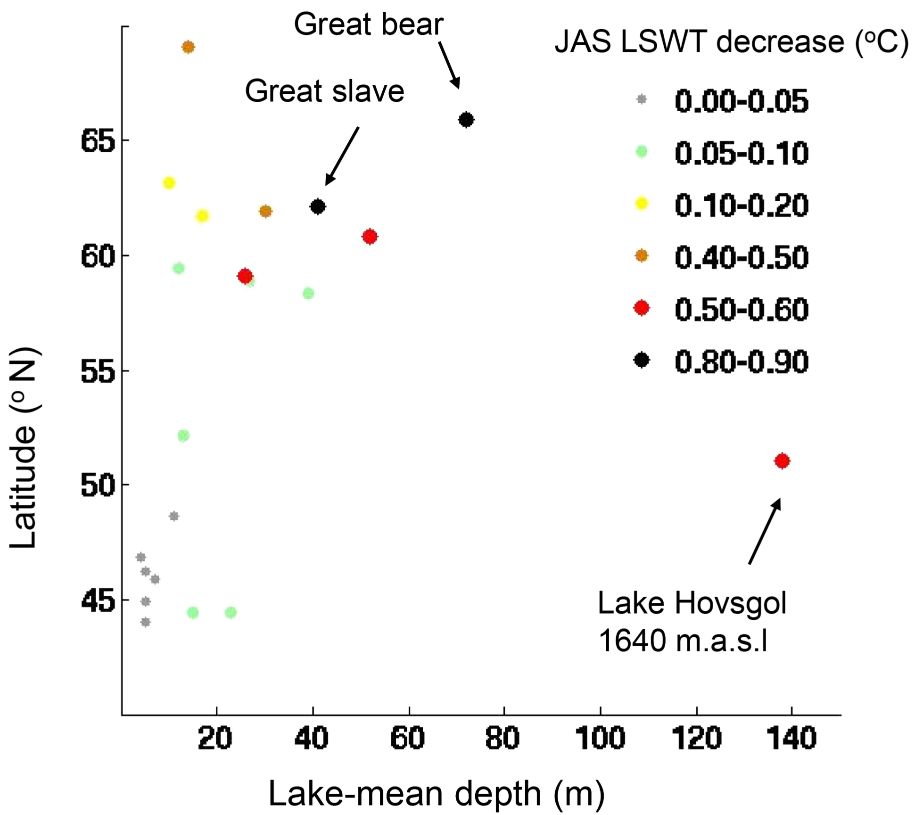

Figure 15. The JAS LSWT decrease (shown as °C decrease per week of later 1 °C warming day) caused by a higher albedo for the 21 trial lakes shown with respect to lake depth and latitude. This figure shows that high latitude and deep lakes show largest JAS LSWT decrease with later 1 °C warming day, signifying that the LSWT of high latitude and deep lakes are more responsive to changes in the 1 °C warming day.

GMDD
8, 8547–8606, 2015

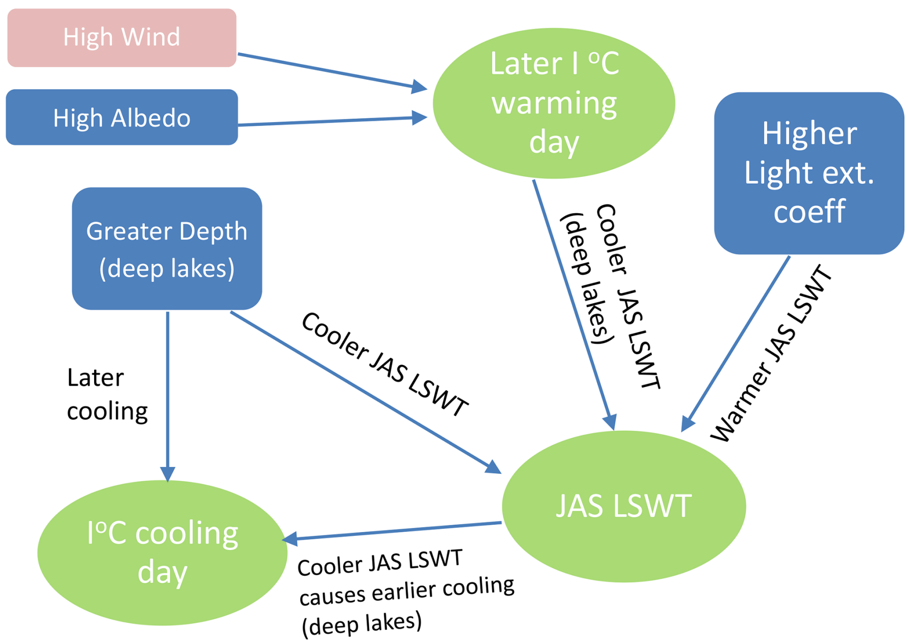

Figure 16. Schematic linking the interactions between the LSWT regulating parameters (blue squares) and wind with the LSWT phases (green circles).

GMDD
8, 8547–8606, 2015

Determining LSWTs worldwide

A. Layden et al.

Title Page
Abstract Introduction
Conclusions References
Tables Figures
◀ ▶
◀ ▶
Back Close
Full Screen / Esc
Printer-friendly Version
Interactive Discussion

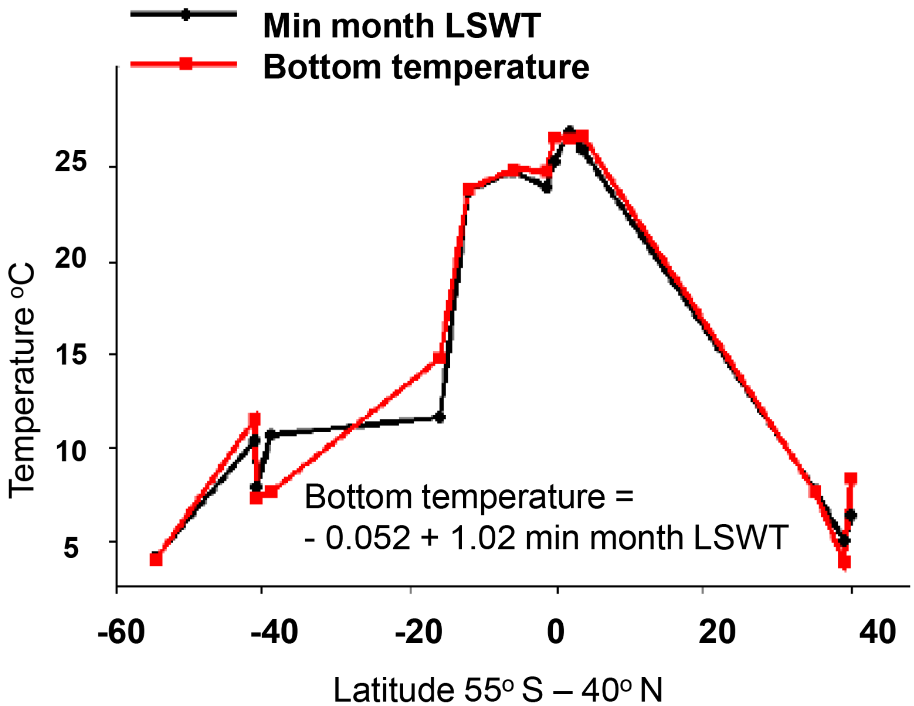

Figure 17. Lake bottom temperature during stratification and climatological monthly minimum LSWT of 14 deep (> 25 m) non-seasonally ice covered lakes from 55° S to 40° N, showing the modelled equilibrium result (lake bottom temperatures obtained from Flake lake model, using perpetual hydrological year, 2005/06) compared with observed monthly minimum climatology LSWTs from ARC-Lake.

GMDD
8, 8547–8606, 2015

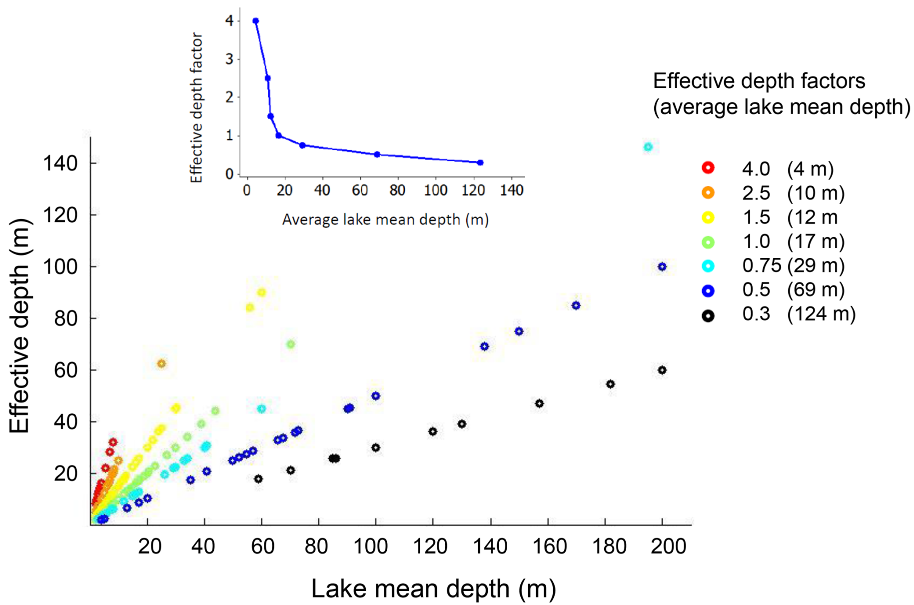

Figure 18. The lake mean depth vs. the modelled effective depth for 244 tuned lakes, colour coded by the effective depth factors and the average lake depth for each effective depth factor used in the tuning process (insert), demonstrating that deeper lakes are tuned to a lower effective depth and shallower lakes to a greater effective depth.

GMDD
8, 8547–8606, 2015

Determining LSWTs worldwide

A. Layden et al.